Activated Murine Thymic Plasmacytoid Dendritic Cells alter Thymopoiesis

by

Alexis Chiana Schmidt

A dissertation submitted to the Graduate Faculty of
Auburn University
in partial fulfillment of the
requirements for the Degree of
Doctor of Philosophy

Auburn, Alabama
August 9, 2010

Approved by

Calvin M. Johnson, Chair, Professor of Pathobiology
Vicky van Santen, Professor of Pathobiology
Bruce F. Smith, Professor of Pathobiology
Jennifer A. Spencer, Instructor of Pathobiology
Tatiana I. Samoylova, Associate Research Professor of Pathobiology
Terry Brandebourg, Assistant Professor of Animal Sciences

Abstract

Pediatric human immunodeficiency virus-1 (HIV-1) infection is characterized by rapid disease progression and profound thymus insufficiency; however the pathogenesis of thymus dysfunction during HIV infection is complex and poorly defined. A recently proposed mechanism for HIV-associated thymus dysfunction is the inhibition of thymopoiesis due to aberrant expression of IFN-α and pro-inflammatory cytokines by activated plasmacytoid dendritic cells (pDC) in the thymic microenvironment. We tested the hypothesis that the products of virus-activated pDC would inhibit or alter thymopoiesis. Thymic pDC were enriched and isolated from 3 week old ICR mice using density gradient centrifugation and magnetic separation using an antibody recognizing m-PDCA-1, a unique marker for murine pDC. pDC represented 0.12% of total thymocytes and 12% of magnetically sorted cells. The phenotype of thymic pDC was found to be $CD4^{+}CD11c^{+}CD123^{+}$m-$PDCA\text{-}1^{+}$. Murine pDC and non-pDC cells were stimulated with the TLR9 ligand CpG for 6 and 24 hours. Supernatant and RNA were collected at each time point and analyzed for expression of IFN-α, TNF-α, and IL-6 using ELISA and RT-PCR. Enriched thymic pDC secreted higher levels of TNF-α, IFN-α and IL-6 than non-pDC at 24 hours post-stimulation. mRNA for TNF-α and IL-6 peaked at 6 hours. To assess the impact of pDC activation on thymopoiesis, murine thymus lobes were obtained at embryonic day 20 or at birth and established in thymus organ culture (TOC). Conditioned media from stimulated and unstimulated pDC were added to TOC; controls

included organ cultures that received normal medium or CpG. Murine TOC that received conditioned media from stimulated pDC tended to have a reduced percentage of $CD4^+CD8^+$ thymocytes and had a significant increase in percentage of $CD4^+CD8^-$ when compared with TOC grown in unconditioned medium or organ cultures directly stimulated with CpG.

These data suggest that the products of activated pDC can induce changes in thymopoiesis that could contribute to thymus dysfunction during immunosuppressive lentivirus infections, even in the absence of virus replication.

Acknowledgments

I would like to thank my advisor, Dr. Calvin M. Johnson, for his guidance and unending support during my time at Auburn University. Additionally, I would like to thank my committee members, Dr. Vicky van Santen, Dr. Bruce Smith, Dr. Jennifer Spencer, and Dr. Tatiana Samoylova for their valuable feedback on my graduate studies. Also, special thanks to Dr. Terry Brandebourg, for serving as my outside reader. I am grateful to Dr. Sandra Ewald who was an original committee member and offered important counsel. The use of murine tissues would not have been possible without the reliable assistance of Dr. Michael Irwin and the permission of Dr. Carl Pinkert. I am appreciative to Allison Church Bird and Dr. R. Curtis Bird for their support in analysis of flow cytometry samples. Without a doubt, I am indebted to Dr. Chengming Wang for his assistance and guidance in so many areas in the lab, in particular PCR and ELISA. I would also like to thank and recognize my high school microbiology teacher, Mrs. Rose Hanscom, who inspired in me a tremendous interest in all things microbiology and introduced me to the book “Microbe Hunters.”

Lastly, I would like to acknowledge my family, my mother Susan, my sister Orian, and my husband Steve, who have supported me and been my cheerleaders.

Table of Contents

List of Tables

List of Figures

List of Abbreviations

CLP	common lymphoid progenitor(s)
CMP	common myeloid progenitor(s)
DC	dendritic cell(s)
FACS	fluorescence activated cell sorting
FBS	fetal bovine serum
FIV	Feline immunodeficiency virus
HEV	high endothelial venules
HIV-1	Human immunodeficiency virus 1
IDC	interdigitating dendritic cells
IFN	Interferon
IL-6	Interleukin 6
IRF	interferon regulatory factor
MACS	magnetic cell sorting
mDC	myeloid dendritic cells
m-PDCA-1	murine-pDC antigen 1
NIPC	Natural interferon-α producing cells
ODN	oligodeoxynucleotides
pDC	plasmacytoid dendritic cell(s)
SLE	systemic lupus erythematosus

TLR	Toll-like receptor(s)
TNF-α	tumor necrosis factor alpha
TOC	thymus organ culture

CHAPTER 1

INTRODUCTION AND REVIEW OF LITERATURE

Introduction

Despite over 25 years of progress in defining the pathogenesis of HIV-AIDS, the worldwide HIV epidemic will soon surpass 40 million people. The rapidly progressive nature of pediatric HIV infection when compared with adult infection is attributable to the thymic role as a centralized site for T-cell loss. Thymocyte depletion during pediatric HIV infection occurs through both direct killing of infected thymocytes and indirect loss due to destruction of the thymic microenvironment. One alteration of the microenvironment suggested from the studies of the feline immunodeficiency virus (FIV) animal model is the abnormal induction of IFN-α, produced by activated plasmacytoid dendritic cells (pDC). Plasmacytoid dendritic cells represent a distinct subset of dendritic cells and are key inducers of the innate immune response to viral infection through the production of type I interferons (IFN-α or IFN-β) and proinflammatory cytokines.

We propose a pathogenetic mechanism in which the innate immune response of the thymic pDC to HIV infection may exert a detrimental effect on thymopoiesis through the aberrant expression of cytokines within the thymic microenvironment. We show herein that such a mechanism inhibits thymopoiesis in a murine thymus model.

A murine thymus model provides an ideal system to study the precise role of activated pDC on thymus function, as reagents are readily available for pDC isolation and functional characterization. We hypothesized that activated pDC will produce factors including the cytokines IFN-α, TNF-α, and IL-6 that alter thymopoiesis. This research will test our larger hypothesis that viruses such as HIV can interrupt T-cell production through a modification of the thymic microenvironment.

The first chapter of this dissertation reviews plasmacytoid dendritic cells (pDC), and their role in normal thymopoiesis, in HIV-1 infection, and in autoimmune diseases. In addition, this chapter examines HIV-1 pathogenesis in the thymus.

The second chapter of this dissertation describes a refined method for the isolation and enrichment of thymic plasmacytoid dendritic cells using a serial process of enzymatic digestion, buoyant density centrifugation, and fluorescence activated and magnetic cell sorting.

The third chapter of this dissertation describes the stimulation of thymic pDC with TLR ligands and the changes in cytokine production following stimulation. We report changes in cytokine production following TLR ligand activation and phenotypic changes in thymocytes following TLR ligation.

The fourth chapter of this dissertation describes the evaluation of the effects of activated pDC on thymopoiesis and the thymic microenvironment. We report the influence of activated pDC on developing thymocytes in murine thymus organ culture and the phenotypic changes in thymocytes following antibody neutralization of cytokines in supernatant of stimulated pDC on thymus organ culture.

Plasmacytoid dendritic cells

Plasmacytoid dendritic cells (pDC) were first discovered in 1958 by pathologists K. Lennert and W. Remmele (*Acta Haematologica*, 1958) who reported cells with plasma cell morphology in the T cell zone of human lymph nodes. These cells were initially named "T-associated plasma cells." It was found, however, that these cells did not express B cell markers, but did express CD4; and were therefore renamed "plasmacytoid T cells" (Liu, 2005). pDC would eventually overlap and converge with another established cell type; the natural interferon-α producing cell (NIPC). NIPC make up a unique group of cells in the peripheral blood that produce IFN-α in response to viral stimulation (Fitzgerald-Bocarsly and Feng, 2007; Fitzgerald-Bocarsly, 2002). pDC and NIPC were discovered to be one in the same cell with regards to phenotype and type I IFN production, as pDC secreted large quantities of IFN-α after stimulation with herpes simplex virus type 1 (HSV-1) (Fitzgerald-Bocarsly and Feng, 2007).

Plasmacytoid dendritic cells are found in the blood and lymphoid tissues, including lymph nodes, thymus, tonsils, spleen, bone marrow and Peyer's patches (McKenna *et al*., 2005). They develop from CD34+ hematopoietic stem cells and are produced continually from the bone marrow during adult life (Liu, 2005). pDC migrate to the T-cell areas of lymph nodes and inflammatory sites by specific expression of chemokine receptors. pDC express CD62-ligand (L-selectin) and CCR7 which recognize receptors on high endothelial venules (HEV), resulting in the accumulation of pDC around HEV and in the T-cell areas of the lymph node (McKenna *et al*., 2005). Human pDC have a round, lymphoid morphology, resembling plasma cells, and are 8 – 10 μm in

diameter (Grouard *et al*., 1997). The surface phenotype of the human pDC is lin^- $CD4^+CD11c^-MHCII^+CD123^+CD45RA^+$.

The exact developmental pathways and origins of plasmacytoid dendritic cells are not fully understood, but key cytokines for pDC development have been identified. Flt3L is one cytokine necessary for pDC development from hematopoietic stem cells in humans and mice (Liu, 2005). Granulocyte colony-stimulating factor (G-CSF) is another cytokine needed for mobilization of pDC from the bone marrow (Colonna *et al*., 2004). $FLT3^+$ cells within common lymphoid progenitors (CLP) and common myeloid progenitors (CMP) were found to differentiate into myeloid DCs and pDCs in culture and in vivo (Naik *et al*., 2005). The common lymphoid origin of pDC is supported by their expression of the pre-T cell receptor α (pTα), λ5, Spi-B, and IgH D-J gene rearrangements (Corcoran, 2003).

pDC are "professional interferon-producing cells" in that they are able to produce 100 to 1000 times more type I IFN than other cell types in peripheral blood mononuclear cells (PBMC) upon viral stimulation (Liu, 2005). Enveloped viruses, double-stranded RNA, and unmethylated bacterial DNA with CpG motifs are all inducers of IFN-α in pDC (Fitzgerald-Bocarsly, 2002). pDC have a unique toll-like receptor (TLR) profile, selectively expressing TLR7 and TLR9 that recognize single-stranded RNA and double-stranded DNA, respectively (Liu, 2005). TLR activation results in the recruitment of adaptor molecules, which activate signaling pathways culminating in gene transcription of IFN-α/β and other proinflammatory cytokines. Induction of type I IFN is regulated by the interferon regulatory factor (IRF) family, made up of nine transcription factors involved in induction of type I IFN and the response to IFN. Transcriptional control of

the IFN-α and IFN-β genes is primarily controlled by IRF-3 and IRF-7, with constitutively high expression of IRF-7 in pDC as compared with myeloid dendritic cells (Colonna *et al*., 2004). Human pDC commit 60% of their transcriptional machinery to type I IFN expression within six hours of viral activation (Ito *et al*., 2006).

Plasmacytoid dendritic cells have emerged as a key cell type in antiviral innate immunity, able to activate and promote the maturation of other cell types through the production of type I IFN. Production of type I IFN by human pDC induces the maturation of myeloid dendritic cells (mDC) through upregulation of costimulatory molecules and secretion of IL-12 (Liu, 2005). NK cells and B cells are also activated through the type I IFN secreted by pDC. B cells are induced to differentiate into virus-specific mature plasma cells (Gilliet *et al*., 2008). Additionally, pDC activate naïve T and Th1 cells through type I IFN (Fitzgerald-Bocarsly and Feng, 2007).

In the steady state, pDC discriminate between host-derived or self DNA and pathogen-derived nucleic acids through the subcellular location of TLR7 and 9 and the methylation of CpG motifs in self DNA. Tolerance to self-DNA is lost in autoimmune diseases such as systemic lupus erythematosus (SLE) and psoriasis. In SLE, immune complexes made up of self-DNA and autoantibodies activate pDC by first binding to the Fc receptor FcγRII (CD32) allowing for internalization of the complex and delivery to TLR9 (Conrad *et al*., 2009). Activated pDC continuously produce type I IFN, found in high levels in the sera of SLE patients, which in turn activate mDC to trigger autoreactive T cells and promote differentiation of B cells into plasma cells (Liu, 2005).
Self-RNA molecules rich in uridine or uridine and guanosine can also trigger pDC to produce type I IFN in SLE through binding with TLR7 (Gilliet *et al*., 2008). In psoriasis,

self-DNA activates pDC by forming large aggregates with the antimicrobial peptide LL37, secreted by damaged epithelial cells (Conrad *et al*., 2009). Self-DNA-LL37 multimeric aggregates are protected from nuclease degradation and are delivered to the early endosomes of pDC where they bind with TLR9 (Gilliet *et al*., 2008). Another host factor found to trigger pDC activation is high-mobility group box 1 protein (HMGB1), a DNA-binding protein released by apoptotic cells that binds to self DNA-LL37 complexes, facilitating their union with TLR9 (Gilliet *et al*., 2008).

Murine pDC were first discovered in 2001 and their phenotype is $CD4^{+}CD11c^{+}B220^{+}lin^{-}CD8\alpha^{-}$ (Asselin-Paturel *et al*., 2001). Murine pDC, like human pDC, respond to viral stimulation with secretion of IFN-α and IL-12 (Bjorck, 2001). Murine pDC also share similar morphology to human pDC, with a characteristic smooth, round shape and eccentric nucleus (Asselin-Paturel *et al*., 2001). Stimulation of murine pDC with influenza virus and CpG oligodeoxynucleotides (ODN) resulted in an upregulation of constimulatory molecules and MHC II, with CpG ODN stimulation providing the strongest pDC activation (Asselin-Paturel *et al*., 2001). Frequency of pDC varies in immune organs and also mouse strains, with a higher frequency of spleen pDC found in 129Sv and the lowest frequency in C57/B6 mice (Asselin-Paturel *et al*., 2003). Murine pDC subsets are delineated with the surface markers CD4, CD8 and Ly49Q, including splenic pDC which are heterogeneous for CD4 and CD8 (Naik *et al*., 2005). Murine pDC also uniquely express Ly49Q, a lectin-type killer cell inhibitory receptor, notably at developmental stages in the bone marrow (Omatsu *et al*., 2005).

Thymic plasmacytoid dendritic cells (pDC)

Hematopoietic progenitor cells give rise to thymic pDC during fetal development, and are found in the medulla and at the cortico-medullary junction (Bendriss-Vermare *et al*., 2001). While pDC are established as interferon-producing cells important in the innate immune response, their function in the thymus has yet to be elucidated. They appear to serve as effectors of innate immunity in the thymus through the production of type I IFN and other cytokines. Plasmacytoid DC are just one subset of dendritic cells populating the thymus, also including myeloid dendritic cells (mDC) and interdigitating dendritic cells (IDC). Each dendritic cell subpopulation is distinct both phenotypically and functionally. Murine pDC are $CD11c^{int}B220^{+}$, compared with myeloid thymic DC which are $CD11c^{hi}$ (Okada *et al*., 2003.). Bendriss-Vermare *et al*. (2001) showed that thymic pDC developed into myeloid DC when cultured with IL-3 and CD40L, as seen with an upregulation of CD86, induction of DC-LAMP, and increased capacity for T-cell stimulation. Thymic pDC express CD2, CD5 and CD7 at intermediate levels, and high levels of IL-3Rα and pre-Tα mRNA (Res *et al*., 1999).

Induction of Type I Interferons in pDC

Type I interferons (IFN) are a family of cytokines made up of IFN-α (multiple subtypes), -β, -ε, -κ, -ω, -δ, and –τ. Of main interest are IFN-α and –β, as IFN-δ and –τ are not found in humans, and IFN-ε and IFN-κ are expressed in the placenta and keratinocytes, respectively (Theofilopoulos *et al*., 2005.). In the human genome, there are 13 IFN-α genes, 1 IFN-β gene, and 1 IFN-ω gene, all lacking introns and found on the short arm of chromosome 9 (Samuel, 2001). Almost all nucleated cells produce type I

IFN in response to viral infection, although pDC produce up to 1000-fold more type I interferon (Theofilopoulos *et al*., 2005.). In both, the mouse and human, there are multiple subtypes of IFN-α and a single IFN-β and IFN-ω that use a common heterodimeric receptor, IFNAR-1 and IFNAR-2, found ubiquitously on most cells (Theofilopoulos *et al*., 2005). Upon IFN-α/β receptor ligation, signaling begins through two tyrosine kinases, Tyk2 and Jak1, which interact with IFNAR-1 and IFNAR-2 receptor subunits respectively (Samuel, 2001). Activation of the receptor-associated enzymes leads to phosphorylation of transcription factors STAT1 and STAT2 (signal transducer and activators of transcription) (Biron, 2001). STAT1 and STAT2 dimerize and complex with IRF9, and this complex, ISGF3, translocates to the nucleus and binds to regulatory sequences in promoter regions of ISG (IFN-stimulated genes) (Biron, 2001). Type I IFNs induce the expression of hundreds of ISGs, which are characterized by antiviral and antiproliferative roles (Haller *et al*., 2007). IRF7 is one such ISG that binds to the promoter region of *IFN-α*, inducing expression of IFN-α, thereby creating a positive feedback loop (Pitha and Kunzi, 2007).

Numerous genes are regulated by type I IFN to create an antiviral state in cells, each targeting a specific point in the viral life cycle. Prominent IFN-induced proteins include the protein kinase PKR, 2',5'-oligoadenylate synthetase (OAS)/RNase L, Mx GTPase, enzyme adenosine deaminase (ADAR), and apolipoprotein B mRNA-editing enzyme catalytic polypeptide-like 3G (APOBEC3G) (Katze *et al*., 2002). PKR is a RNA-dependent protein kinase that is activated by double and single-stranded RNA to phosphorylate several substrates, including the α subunit of the protein synthesis factor eIF-2 (Samuel, 2001). Serine phosphorylation of eIF-2α impairs the catalytic function of

eIF-2B, leading to the inhibition of translation initiation. 2-5A synthetase (OAS) and RNase L are two enzymes in a key pathway that degrades RNA in the cell after induction of interferon. OAS synthesizes oligomers of adenosine linked by phosphodiester bonds, and these oligoadenylates bind and subsequently activate RNase L, a latent endoribonuclease (Silverman, 2007). The active RNase L protein degrades both viral and cellular rRNA, through cleavage of single stranded regions (Silverman, 2007). The Mx pathway is another key pathway in the IFN-induced antiviral state. Mx proteins are members of the dynamin family of GTPases, which target viral nucleocapsids and viral RNA synthesis (Samuel, 2001). Another IFN-induced protein is the enzyme ADAR1, a RNA-specific adenosine deaminase which edits RNA by deaminating adenosine to yield inosine, leading to altered cellular and viral RNA transcripts (Samuel, 2001). An important nucleic-acid editing enzyme induced is apolipoprotein B mRNA-editing enzyme catalytic polypeptide-like 3G (APOBEC3G), a member of the cytidine deaminase family of enzymes. APOBEC3G converts cytosine residues in viral DNA to uracil, resulting in mutations in proviral DNA (Argyris and Pomerantz, 2004). Interestingly, APOBEC3G is an inhibitor of HIV-1 Vif, although wild-type HIV-1 Vif counteracts this activity through binding APOBEC3G and targeting it for degradation (Argyris and Pomerantz, 2004).

Induction of Pro-inflammatory cytokines TNF-α and IL-6

TNF-α and IL-6 are two key pro-inflammatory cytokines that direct the host's response to infection (Janeway *et al*., 2005). TNF-α, produced by macrophages, activates endothelial cells in blood vessels to express adhesion molecules, including ICAM-1 that

promote and facilitate the binding of circulating monocytes and leukocytes (Janeway *et al*., 2005). Additionally, TNF-α secreted by macrophages induces blood clotting in order to contain the infection. TNF-α and IL-6 are endogenous pyrogens that act on the hypothalamus to elevate the body's temperature during infection. Both cytokines initiate the acute-phase response, acting on the liver to synthesize acute-phase proteins, such as C-reactive protein, which opsonize pathogens and trigger the complement cascade (Janeway *et al*., 2005). If TNF-α is released systemically, in the case of a systemic bacterial infection, vasodilation and increased vascular permeability occur and lead to septic shock (Janeway *et al*., 2005).

TNF-α is a member of the Tumor Necrosis Factor superfamily of cytokines that activate signaling pathways related to cell homeostasis, death and differentiation. It is a 17-kd homotrimeric protein, encoded within the major histocompatibility complex (MHC), found in both membrane and soluble forms. Members of the TNF superfamily can bind and interact with one or more cognate receptors. TNF-α interacts with receptors TNFR1 (p55) and TNFR2 (p75), expressed on all somatic cells (Ware, 2003). The cytoplasmic tail of TNFR1 contains a death domain and subsequent binding of TNF-α with TNFR1 leads to apotosis (Ware, 2003). TNFR2 lacks a death domain, and TNF-α binding leads to cell survival and inflammation (Ware, 2003).

TNF-α and IL-6 are primarily produced by macrophages, monocytes, and T cells. Both cytokines are also produced by plasmacytoid dendritic cells (pDC) when activated through ligation of TLR7 or TLR9 (Gilliet *et al*., 2008). Signaling occurs through adaptor molecules that come together to make a complex that activates the transcription factor NF-κB, which induces gene transcription of TNF-α and IL-6. Murine pDC

produce TNF-α and IL-6, in addition to other cytokines, in response to HSV-1 and synthetic oligodeoxynucleotides (Hochrein *et al*., 2004). Omatsu *et al*. (2005) found immature pDC and mature pDC in bone marrow, characterized by their expression levels of Ly49Q, produced high levels of TNF-α, IL-6, IL-12 p70, and IFN-α when exposed to CpG-oligodeoxynucleotides. Interestingly, $Ly49Q^-$ pDC produced less IL-6, IL-12 and IFN-α than $Ly49Q^+$ pDC, but comparable levels of TNF-α. The authors purport that $Ly49Q^-$ pDC are at a different stage of differentiation than $Ly49Q^+$ pDC, and this may be a possibility in other tissues as $Ly49Q^-$ pDC are found in blood, thymus and nonlymphoid tissues (Omatsu *et al*., 2005). Veckman and Julkunen (2008) showed that human pDC produce TNF-α, IL-6, and IFN-α in response to stimulation with live *Streptococcus pyogenes*. Cytokine levels produced by *S .pyogenes*-stimulated pDC were similar when compared with levels of TNF-α and IL-6 produced by influenza A virus-infected pDC (Veckman and Julkunen, 2008).

Toll-like receptors (TLRs)

Toll-like receptors (TLRs) are one group of pattern recognition receptors (PRR) that recognize evolutionarily conserved molecular patterns found in bacteria and viruses. These immune receptors are essential members of the innate immune system, and ten have been discovered in humans while thirteen TLRs have been found in the mouse (Bowie and Haga, 2005). TLR ligation leads to a complex signaling cascade that induces transcription of antiviral proteins and pro-inflammatory cytokines.

TLRs are transmembrane proteins with shared homology in their ectodomain to interleukin-1 receptors (IL-1Rs) (Cook *et al*., 2004). This Toll-IL-1R (TIR) domain is

comprised of approximately 18 to 25 tandem copies of a leucine-rich motif (Kim *et al*., 2007). TLR signaling is mediated through this TIR domain and the adaptor molecule MyD88 (myeloid differentiation primary response protein 88). Members of the TLR family that recognize flagellin and lipoproteins, found in bacteria and fungi, include TLR1, TLR2, TLR4, TLR5 and TLR6 and are located on the plasma membrane (Saitoh and Miyake, 2009). Remaining members, including TLR3, TLR7, TLR8, and TLR9, recognize nucleic acids and reside intracellularly in endosomes and lysosomes (Saitoh and Miyake, 2009). Toll-like receptors signal through adaptor proteins that interact with the TIR domain; all TLRs use MyD88 as an adaptor protein except TLR3 which uses TRIF (TIR domain-containing adaptor protein inducing IFNβ) (Barton and Kagan, 2009). The binding of adaptor proteins begins a signaling cascade that ultimately results in the phosphorylation of IκB, which releases the transcription factor NF-κB to translocate to the nucleus to induce transcription of pro-inflammatory cytokines and costimulatory molecule genes (Cook *et al*., 2004). TLRs also activate interferon regulatory factors IRF-3 and IRF-7, transcription factors that regulate expression of type I IFN. IRF3 is constitutively expressed and induces early transcription of IFN-β, whereas IRF7 is activated through expression of IFN-β and responsible for induction of IFN-α and IFN-β genes (Taniguchi *et al*., 2001).

TLR3, TLR7, TLR8 and TLR9 are unique in their recognition of microbial nucleic acids and localization in intracellular compartments. TLR9 resides in the endoplasmic reticulum (ER) of unstimulated dendritic cells and macrophages, and travels to lysosomes following internalization of CpG-DNA (Latz *et al*., 2004). Another report has shown that UNC93B1, a resident ER protein, plays a crucial role in delivery of TLR7

and TLR9 to endolysosomes (Kim *et al*., 2008). In mice engineered with a mutation in UNC93B1, TLR7 and TLR9 remain in the ER following stimulation compared with wild-type mice (Kim *et al*., 2008).

Toll-like receptors are receiving increased attention as they may play roles in the development of systemic autoimmune diseases such as systemic lupus erythematosus (SLE), scleroderma, and rheumatoid arthritis (RA). TLR7 and TLR9, expressed exclusively by pDC, can bind endogenous ligands, including immune complexes containing DNA and RNA found in SLE. pDC express Fc receptors which bind IgG-immune complexes, and internalize the complexes delivering them to endolysosomes where TLR7 and TLR9 receptors are recruited (Marshak-Rothstein, 2006). Endogenous nucleic acids originate from dead or dying cells and subsequently stimulate the production of autoantibodies by reactive B cells (Marshak-Rothstein, 2006.).

Pathogenesis of HIV-1 in the thymus

A unique element in the pathogenesis of HIV infection of children is the vulnerability of the thymus to productive infection at its height of physiologic activity (Gaulton *et al*., 1997). Infection of this central lymphoid tissue disrupts thymopoiesis through multiple mechanisms and induces regional inflammation (Haynes *et al*., 2000). HIV-1 infection and the progression to AIDS are primarily characterized by the decline of CD4+ T cells and a failure to maintain the T cell repertoire. The development of naïve T cells occurs in the thymus during fetal development and the neonatal period, establishing a comprehensive peripheral T cell repertoire. Reports have shown the impaired production of naïve T cells in HIV-1 infected patients, suggesting that thymic

function is suppressed by HIV-1. In fact, the thymus is an early site for HIV-1 infection, and thymocytes are uniquely vulnerable to lytic viral infection (Meissner *et al*., 2003).

The normal human thymus will begin to atrophy at puberty, and this process is characterized by an increase in the perivascular space and a decrease of the thymic epithelial space (Haynes *et al*., 2000). The HIV-1 infected thymus of children undergoes premature atrophy and develops a concerted lymphoid infiltrate in the perivascular spaces (Haynes *et al*., 2000). Other morphological changes induced by HIV-1 infection in the thymus include a loss of Hassall's corpuscles and a condensation of the thymic epithelium (Gaulton *et al*., 1997).

Thymic injury and loss of thymic function due to HIV-1 infection is the combined result of at least two broad mechanisms. First, thymocytes are depleted due to direct lysis of HIV-1 infected cells. Expression of CD4, the primary receptor for HIV, is found on immature and mature thymocytes and intrathymic T progenitor cells (ITTP), rendering these cells vulnerable to viral infection (McCune, 1997). Besides direct infection, thymocytes are also depleted by indirect mechanisms as evidenced by paracrine effects of molecules (including IFN-α and IL-10) secreted by aberrantly activated or infiltrating cells (Meissner *et al*., 2003). All thymocytes express the IFN-α receptor β chain (CD118), and are potentially responsive to secretion of IFN-α by thymic pDC as a consequence of innate immune stimulation. Sustained activation of pDC could impair thymopoiesis by disrupting the thymic microenvironment. In support of this theory, Schmidlin *et al*. (2006) reported that endogenous IFN-α produced by activated pDC impaired the T cell development of human $CD34^{+}CD1a^{-}$ thymic progenitor cells, while exogenous IFN-α impaired the upregulation of specific surface markers associated with T

cell development in a dose-dependent manner. Furthermore, type I interferons have been reported to induce terminal differentiation and subsequent apoptosis of uninfected thymic epithelial cells (TEC) in vitro (Vidalain *et al*., 2002) and after measles virus infection (Vidalain *et al*., 2002).

Role of pDC in HIV infection

The field of dendritic cell biology has evolved as dendritic cells play important roles in both the innate and acquired immune responses (Steinman and Hemmi, 2006). They also provide protection from pathogens through their expression of pattern recognition receptors (PRR), including TLR and C-type lectins. Dendritic cells play several roles in the pathogenesis of HIV, and the role of plasmacytoid dendritic cells is characterized by the secretion of type I IFN in response to HIV infection.

Plasmacytoid DC express CD4, the primary receptor for HIV, and chemokine receptors CCR5, and CXCR4, the co-receptors utilized by the virus (Muller-Trutwin and Hosmalin, 2005). Reports have shown peripheral blood pDC are susceptible to HIV infection in vitro and in vivo (Schmidt *et al*., 2005). HIV was isolated from purified blood pDC of a HIV-infected individual after culture with IL-3 and CD40L (Schmidt *et al*., 2005). Patterson *et al*. (2001) had also shown both mDC and pDC from blood could be infected by HIV-1 in vitro, with the virus replicating more efficiently in pDC compared with mDC. Schmidt et. al.(2004), however, reported limited virus replication in pDC despite their infection by HIV-1 isolates utilizing either CCR5 or CXCR4 coreceptors. When antibodies to IFN-α were added to HIV-stimulated pDC plus CD40L, viral replication increased by three fold (Schmidt *et al*., 2005). pDC produce large

amounts of IFN-α in response to HIV-1 within 48 hours, and secretion of IFN-α is not limited by heat-inactivated HIV-1 strains (Yonezawa *et al*., 2003). Furthermore, exposure to HIV-1 also results in the differentiation and maturation of blood pDC (Schmidt *et al*., 2005). This differentiation includes morphological changes into classical dendritic cells with dendrites. Additionally, pDC cultured with HIV-1 upregulated maturation markers CD80 and CD86 (Yonezawa *et al*., 2003). Fonteneau *et al*. (2004) found that pDC exposed to nonreplicative HIV-1 strongly upregulated maturation markers CD83 and CCR7, while only slightly upregulating CD80 and CD86. Myeloid DC did not mature as a consequence of exposure to HIV-1; however, mDC did differentiate and upregulate maturation markers when cultured with HIV-1-stimulated pDC (Fonteneau *et al*., 2004).

Evidence has shown that dendritic cells are reduced and their function is abated during HIV infection. A number of groups have reported decreased numbers of blood pDC and blood $CD11c^+$ mDC in HIV-infected individuals and AIDS patients (Chehimi *et al*., 2002, Soumelis *et al*., 2001, Donaghy *et al*., 2001, Feldman *et al*., 2001, Schmidt *et al*., 2004). Surprisingly, Soumelis *et al*. (2001) found that blood pDC numbers were increased in asymptomatic long-term survivors (LTSs) and they had significantly lower viral loads compared with patients with low numbers of pDC. The progressive depletion of pDC correlated with an increasing HIV-1 plasma viral load (Donaghy *et al*., 2001; Schmidt *et al.*, 2005). Myeloid DC are also reduced in HIV-infected subjects as reported by a number of groups (Donaghy *et al*., 2001; Feldman *et al*., 2001; Schmidt *et al*., 2005). The exact mechanism of depletion of these two dendritic cell subsets remains unclear. One plausible mechanism for the loss of blood pDC in HIV-infected

individuals, is their subsequent migration to secondary lymphoid tissues and maturation following exposure to the virus. Another possibility for the loss of pDC and mDC is direct infection by HIV-1, as both DC subsets express CD4. Loss of IFN-α production by pDC during primary HIV-1 infection affects viral replication and activation of other cell types in the immune system. Studies report an impairment in function of blood pDC of HIV-infected patients, as shown by a decreased response to viral stimulation and less IFN-α (Feldman *et al*., 2001). IFN-α regeneration during immune restoration of HIV-infected patients on antiretroviral therapy (ART) was associated with resistance to opportunistic infections (Siegal *et al*., 2001).

In summary, there is ample experimental evidence to indicate that pDC are a crucial component of the innate immune response to HIV infection. Their distribution throughout the thymus further suggests that pDC play a role in normal thymus function, and possibly, induction of thymic involution. However, the precise role of pDC activation on thymopoiesis has not been determined. Therefore, we sought to develop an ex vivo system in which to characterize the products of pDC activation and the impact of activation on thymopoiesis.

CHAPTER 2

ENRICHMENT OF PLASMCYTOID DENDRITIC CELLS FROM THE MURINE THYMUS

Introduction

Plasmacytoid dendritic cells (pDC) comprise approximately 0.2% of hematolymphoid cells in the human thymus (Gurney *et al*., 2004). Despite their small numbers, much research has shown that pDC play an integral role bridging innate and adaptive immunity. While numerous studies have focused on blood pDC, fewer groups look to examine pDC in the lymphoid tissues. This is due to the fact that pDC are a subset of dendritic cells, and, therefore, must be distinguished from conventional or myeloid dendritic cells using cell-surface markers and their histologic localization. Within most secondary lymphoid tissues, pDCs are localized around high endothelial venules (HEV) and T-cell rich areas (Grouard *et al*., 1997); human blood pDC express L-selectin (CD62-L) in order to emigrate into lymph nodes through high endothelial venules (Colonna *et al*., 2004). Key cell-surface markers that distinguish pDC from mDC include CD123 (IL-3Rα), BDCA-2 (Dzionek *et al*., 2001) and DLEC the latter two only present on human pDC.

Plasmacytoid dendritic cells are found in the thymus, although their precise role in the thymus remains unknown. Using immunohistochemistry, Schmitt *et al*. (2007) determined pDC were localized in the medulla of the thymus. In the mouse, unlike in the

human, both dendritic cell subsets, mDC and pDC, express CD11c (Bendriss-Vermare *et al*., 2001). Additionally murine pDC in the thymus express B220 (CD45R), distinguishing them from myeloid dendritic cells (Okada *et al*., 2003). Okada *et al.* (2003) found the phenotype of the thymic pDC to be $CD11c^{+}B220^{+}CD4^{+/-}CD8\alpha^{+/-}$MHC $I^{+}CD44^{+}Ly6C^{+}MHCII^{lo}$. This chapter describes the protocol developed to isolate and enrich pDC from the murine thymus and the characterization of these cells.

Materials and Methods

Fluorescence activated cell sorting (FACS) enrichment by negative selection

Three to four-week old ICR mice were obtained from an ongoing project in the laboratory of Drs. Carl Pinkert and Mike Irwin. Thymuses were collected under sterile conditions immediately after euthanasia by cervical dislocation and placed in sterile RPMI 1640 medium (Invitrogen, Carlsbad, CA) supplemented with penicillin-streptomycin (Invitrogen, Carlsbad, CA). Thymuses were transferred to a petri dish containing 5 ml RPMI medium, and teased apart using two 22 gauge needles for ten minutes. An enzyme solution of 20 mg/ml DNase I (Roche, Indianapolis, IN) and 1.0 mg/ml Collagenase A (Roche) in 5 ml RPMI medium was added to the disassociated thymic tissue and incubated at 37°C for 30 minutes with gentle rotation. Digested fragments were filtered through a 100 µm Falcon cell strainer with 10 ml RPMI 1640 media containing 5 µg/ml DNase I (Roche). The single-cell suspension was washed twice for 5 minutes at 540 *g* with ice-cold 1X phosphate-buffered saline solution (PBS) supplemented with 5 m*M* EDTA and 5% FBS. The thymocytes were resuspended in cold isotonic Percoll solution (density 1.077 g/ml) at 1.5 x 10^{8} cells/ml. Discontinuous density

gradients were prepared in 15 ml conical tubes by layering 1 ml FBS, 3 ml cell suspension, and 2 ml Percoll solution. Tubes were centrifuged at 1700 *g* for 10 minutes at 4°C. Low-density cells were collected at the interface of the Percoll and FBS from each tube using a cannula. The low-density cells were washed three times with 15 ml PBS supplemented with EDTA and FBS at 540 *g* for 5 minutes. Low density cells were incubated with an antibody cocktail of CD11b-PE, CD19-PE, CD14-PE, CD3-PE and CD8α-PE (all at 20 µg/ml) for 30 minutes in the dark on ice. Cells were washed twice with the addition of 2 ml of flow buffer (1X PBS, 2% FBS, 0.1% sodium azide) followed by centrifugation at 200 *g* for 5 minutes at 4° C. Cells were subsequently sorted to collect the PE-negative fraction using a MoFlo high-speed cell sorter (Dako cytomation) with Summit software. A small fraction of the negatively sorted cells were stained with m-PDCA-1-FITC (Miltenyi Biotec, Auburn, CA) for positive identification of murine pDC by flow cytometry.

Magnetic cell sorting (MACS) enrichment of murine thymic pDC

The thymuses of three to four-week old ICR mice were processed to collect low-density cells as described above. The low-density cells were washed three times with 15 ml PBS supplemented with EDTA and FBS at 540 *g* for 5 minutes. Cells were resuspended in 400 µl MACS buffer (1X PBS supplemented with 2 m*M* EDTA and 0.5% BSA) per 10^8 total cells. Anti-mPDCA-1 Microbeads (Miltenyi Biotec, Auburn, CA) were added at 100 µl per 10^8 cells and incubated for 15 minutes at 4°C. Magnetically labeled cells were washed in approximately 3 ml MACS buffer and centrifuged at 300 *g* for 10 minutes.

The supernatant was aspirated and cells were resuspended in 500 µl MACS buffer per 10^8 cells.

The MS magnetic column (Miltenyi Biotec, Auburn, CA) was primed by the addition of 500 µl MACS buffer. The magnetically-labeled cell suspension was added to the column and unlabeled cells were collected as the negative fraction. The column was then washed three times by adding 500 µl MACS buffer. The column was removed from the magnet and using a new collection tube, magnetically labeled cells were flushed out by adding 1 ml buffer to the column and applying the plunger. Cell counts were performed to determine cell numbers for both negative and positive fractions.

Cell staining of the low density fraction

Low density cells were collected after density centrifugation and adjusted to a concentration of 2 x 10^6 cells/ml. Cells were filtered using a 5 ml polystyrene tube with cell-strainer cap (BD Falcon, Franklin Lakes, NJ) to remove large cell clusters. Cells were stained with monoclonal antibodies against CD11c-PE (0.2 mg/ml) (eBioscience, San Diego, CA), CD4-Alexa647 (0.2 mg/ml BD Pharmingen, Franklin Lakes, NJ) and mPDCA-1-FITC (1:11, Miltenyi Biotec, Auburn, CA). Low density cells were incubated for 30 minutes on ice in the dark. At the end of the incubation, cells were washed twice with the addition of 2 ml flow buffer (1X PBS, 2% FBS, 0.1% sodium azide) followed by centrifugation at 200 *g* for 5 minutes at 4° C. Cells were fixed with equal parts 0.5% paraformaldehyde and flow buffer and incubated for 30 minutes on ice in the dark. Cells were washed as stated above at the end of fixation, and 500 µl flow buffer was added to cells. Cells were analyzed using a MoFlo cytometer and Summit software.

Staining of m-PDCA-1$^+$ cells

m-PDCA-1$^+$ cells were collected from the magnetic column (Miltenyi Biotec, Auburn, CA) and filtered using a 5 ml polystyrene tube with cell-strainer cap (BD Falcon, Franklin Lakes, NJ). The cell concentration was adjusted to 1 x 10^6 or 2 x 10^6 cells/ml depending on the total number of cells. Cells were stained with antibodies against IgG-PE (BD Pharmingen, Franklin Lakes, NJ), CD4-Alexa 647(BD Pharmingen, Franklin Lakes, NJ), and CD123-FITC (eBioscience, San Diego, CA). Cells were incubated for 30 minutes on ice in the dark. At the end of the incubation, cells were washed twice with the addition of 2 ml of flow buffer (1X PBS, 2% FBS, 0.1% sodium azide) followed by centrifugation at 200 *g* for 5 minutes at 4° C. 500 µl flow buffer were added and cells were kept in the dark. Cells were analyzed using a MoFlo cytometer and Summit software.

Immunofluorescence microscopy

Frozen 5 µm sections of thymus were prepared from a 3 week old ICR mouse using a Microm HM550 cryostat (Richard Allen Scientific, St. Louis, MO). Slides were fixed in ice-cold acetone for 10 minutes on ice. After fixation, slides were washed three times with 1X PBS for 5 minutes each. A blocking solution (0.1X PBS, 5% BSA, 10% FBS) was applied to each slide for 1 hour in a dark humidified chamber. The primary antibody solution, diluted 1:25 in blocking buffer, was added to the slides and incubated for 1 hour at room temperature in a dark humidified chamber. Following incubation, slides were washed three times as stated previously. A DAPI counterstain, diluted to 300 nM, was applied to each slide for 30 minutes at room temperature in a dark humidified chamber. Slides were washed three times as previously stated. Lastly, the slides were

mounted and a coverslip was affixed using Citiflour (aqueous polyvinyl alcohol). Slides were viewed and photographed using a Nikon Eclipse E800 microscope (Nikon, Inc., Melville, NY).

Results

Enrichment of pDC

Thymic plasmacytoid dendritic cells (pDC) were isolated and enriched from the murine thymus using both FACS and MACS. The median number of pDC per thymus enriched using FACS was 1.09×10^6, while the median number of pDC per thymus enriched using MACS was 2.35×10^6 (Fig. 1). Using MACS resulted in a significant increase ($p < 0.01$) in total pDC yield per thymus when compared to using FACS. The median percentage of pDC enriched from total thymic cells by FACS was 0.04%, while the median percentage of pDC collected from total thymic cells enriched by MACS was 0.12% (Fig 2). Magnetic cell sorting resulted in a significant ($p=0.01$) increase in pDC yield from total thymic cells when compared with fluorescence activated cell sorting. Considering the beginning frequency of pDC (0.12% of total thymic cells) and the final frequency of 11.6% of the positive magnetic fraction (Table 1), pDC were enriched approximately 100 fold using the MACS protocol.

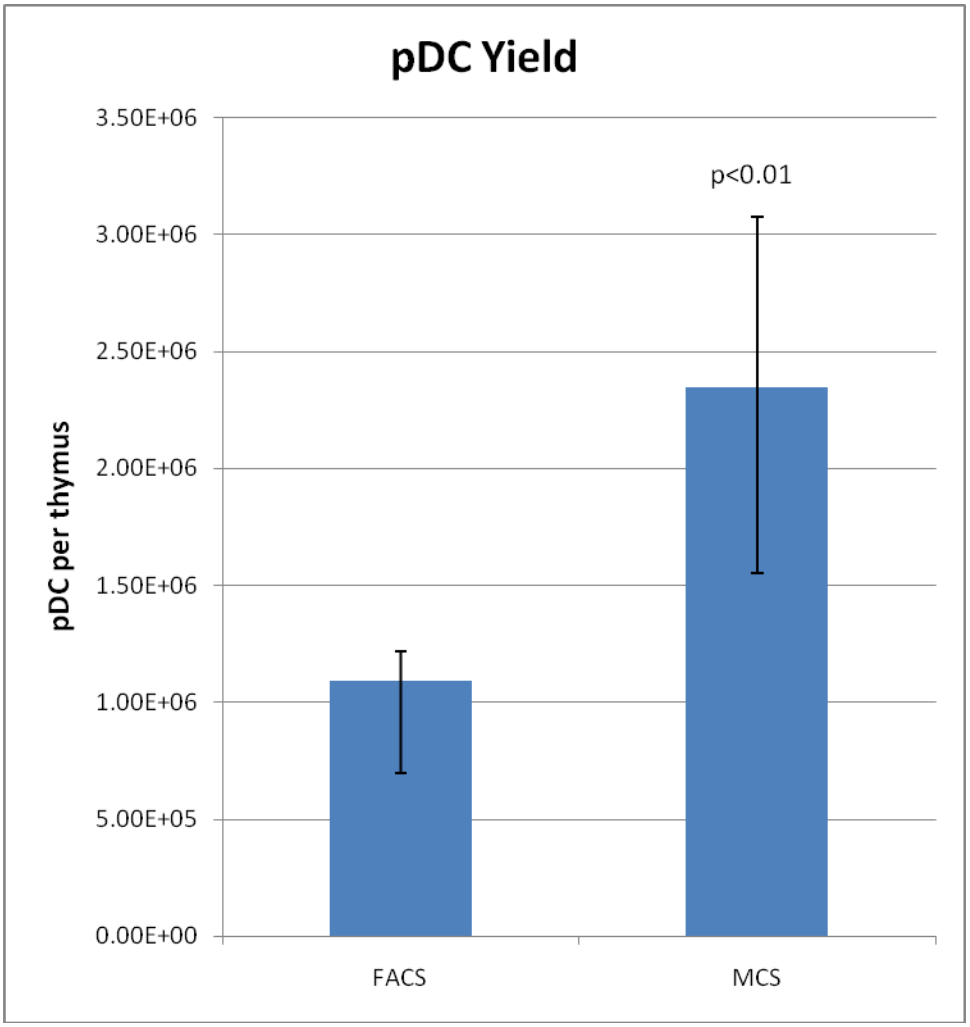

Figure 1. pDC yield per thymus from MACS compared with FACS. Magnetic cell sorting (MCS) resulted in a significant ($p<0.01$) increase in total pDC yield when compared with fluorescence activated cell sorting (FACS). The median number of pDC enriched from each thymus by FACS was 1.09×10^6 ($6.98 \times 10^5 - 1.22 \times 10^6$), while the median number of pDC enriched from each thymus by MACS was 2.35×10^6 ($1.55 \times 10^6 - 3.08 \times 10^6$). Antennae represent the interquartile range for each data set. Medians were compared using the Mann-Whitney U test. MCS indicates MACS. Medians represent n=9 for FACS, and n=16 for MACS.

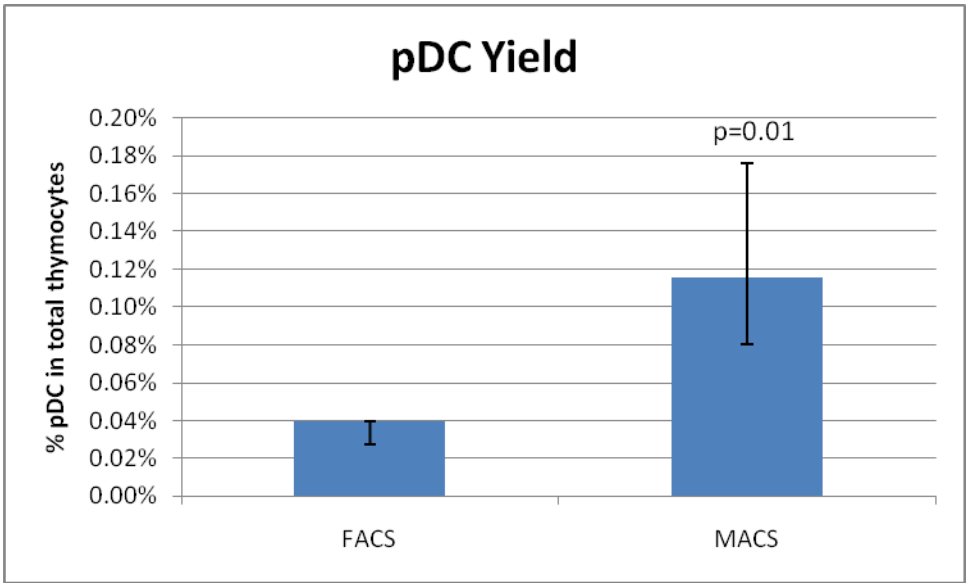

Figure 2. Percentage of pDC in total thymocytes from MACS compared with FACS. Magnetic cell sorting (MACS) resulted in a significant (p=0.01) increase in pDC percentage in the enriched fraction when compared with fluorescence activated cell sorting (FACS). The median percentage of pDC enriched from total thymic cells by FACS was 0.04% (0.03-0.04%), while the median percentage of pDC collected from total thymic cells enriched by MACS was 0.12% (0.08-0.18%). Antennae represent the interquartile range for each data set. Medians were compared using the Mann-Whitney U test. Medians represent n=9 for FACS, and n=16 for MACS.

	Frequency of pDC
Total thymocytes	0.12% (0.04 – 0.43%)
Low density fraction	2.54% (1.12 – 4.37%)
Positive magnetic fraction	11.6%

Table 1. Frequency and range of pDC of total thymocytes, low density fraction, and positive magnetic fraction.

Identification of dendritic cell subsets

Within the low density fraction, two dendritic cell populations were distinguished with the cell-surface markers CD11c and m-PDCA1. Myeloid dendritic cells had the phenotype $CD4^+CD11c^+$m-$PDCA1^-$ and comprised 3.7% of the low density cell fraction. The phenotype of plasmacytoid dendritic cells was $CD4^+CD11c^+$m-$PDCA1^+$ and comprised 1.8% of low density cells (Fig 3B).

Cells positive for m-$PDCA\text{-}1^+$ were also positive for CD4 and CD123 (Fig 4A). m-$PDCA\text{-}1^+$ cells represented approximately 12% of cells in the positive fraction from the magnetic column. m-$PDCA\text{-}1^+CD4^+CD123^+$ cells were backgated in the scatterplot and found to be heterogeneous in terms of size and complexity (Fig 4B).

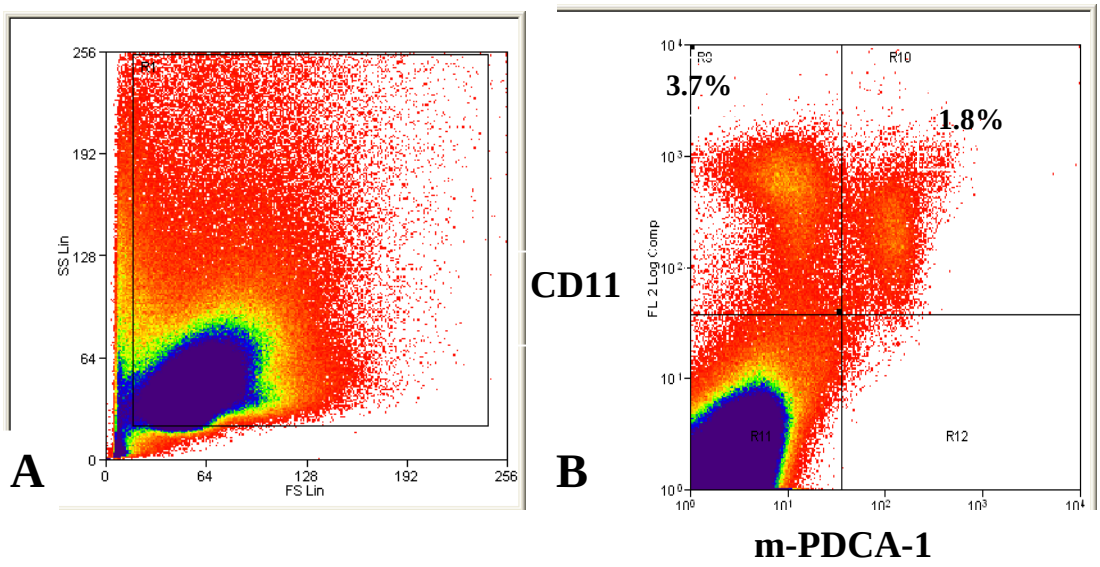

Figure 3. Scatterplot and staining of the low density cell fraction. A) Scatterplot of the low density cell fraction B) Low density cells were gated on $CD4^+$ cells; showing positive staining using m-PDCA1-FITC and CD11c-PE.

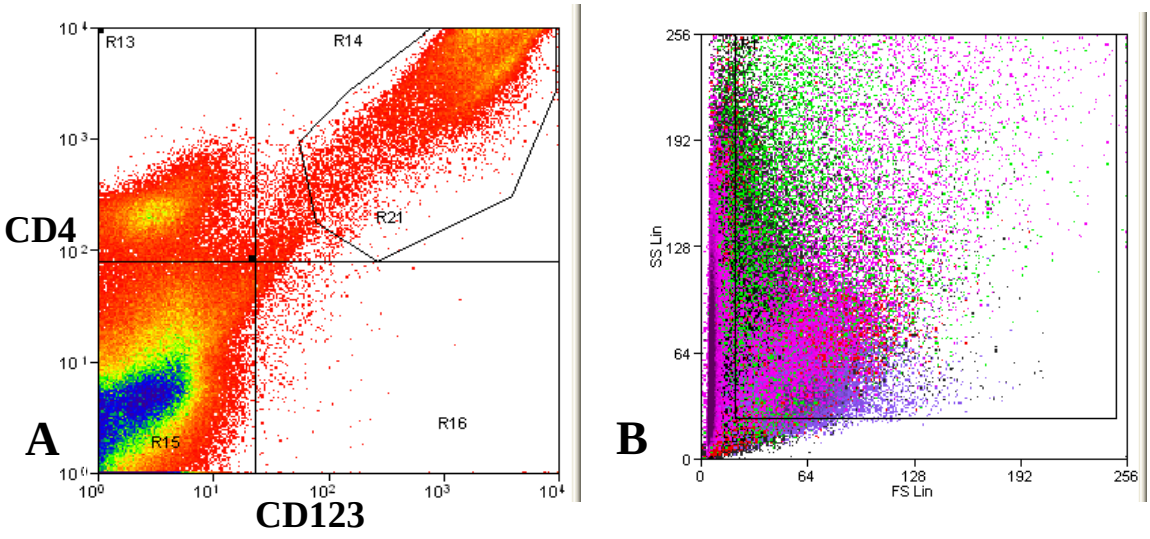

Figure 4. Staining and back gating of m-PDCA-1+ cells. m-PDCA-1^+ cells are $CD4^+CD123^+$, shown in the gated area R21. They are shown in pink in the scatterplot in panel B, indicating a broad range of size (forward scatter) and granularity (side scatter).

Immunofluorescence microscopy of murine thymus

Immunofluorescence staining of frozen murine thymus sections using antibody m-PDCA-1 and DAPI revealed specific fluorescence in the medulla and the cortico-medullary junction, with a pattern showing intense cytoplasmic fluorescence at the cell membrane (Fig 5).

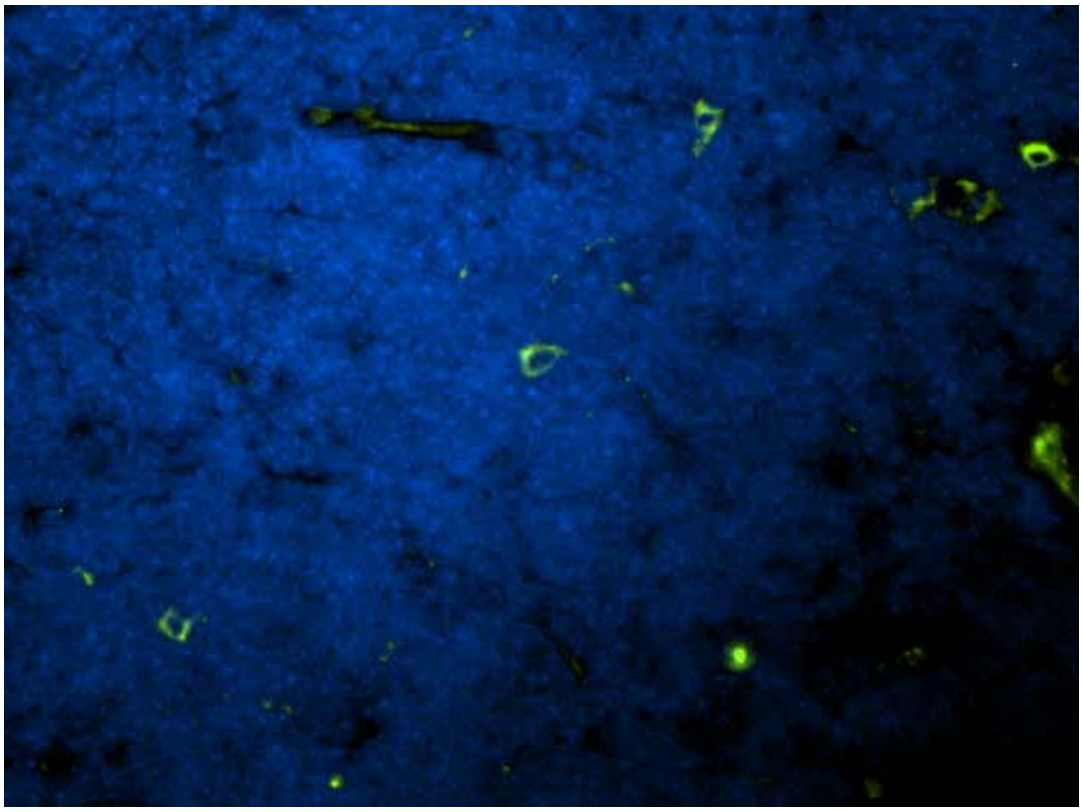

Figure 5. Direct labeling of m-PDCA-1^{+} cells in murine thymus. Thymus sections were stained with monoclonal antibody m-PDCA-1 conjugated to FITC, and counterstained with DAPI.

Discussion

Plasmacytoid dendritic cells (pDC) are found in blood, and numerous tissues, including spleen, lymph nodes, thymus and bone marrow. Their paucity of number in lymphoid tissues requires a precise method of isolation reliant on specific markers and physical characteristics. The frequencies of pDC found in the present study are consistent with previous studies (Asselin-Paturel *et al*., 2001). Here, we utilized both FACS and MACS to enrich and isolate pDC from the murine thymus. pDC were isolated through negative selection using FACS, by removing B cells, monocytes, myeloid dendritic cells, and T cells. pDC enriched with MACS employed positive selection, using the murine-specific marker m-PDCA-1 conjugated to magnetic beads. MACS resulted in a significant increase in total pDC yield per thymus when compared to FACS. Magnetic cell sorting also resulted in a significant increase in pDC yield out of total thymocytes when compared with fluorescence activated cell sorting. To further quantify pDC in low density fraction, cellular staining for CD11c and m-PDCA-1 was employed and identified the two expected dendritic cell populations, pDC and mDC.

Plasmacytoid dendritic cells found in the thymus characteristically are found in the medulla and at the cortico-medullary junction (Bendriss-Vermare *et al*., 2001). The results of our immunofluorescence assay were consistent with Bendriss-Vermare *et al*. (2001) with the localization of pDC in the medulla and along the cortico-medullary junction.

The murine-specific pDC marker murine pDC antigen 1 (m-PDCA-1) is also known as bone marrow stromal antigen 2 (BST2), although little is known about this

marker (Blasius *et al*., 2006). Blasius *et al.* (2006) found that BST2 is localized and cycles between the plasma membrane and Golgi apparatus (Blasius *et al*., 2006).

CHAPTER 3

STIMULATION OF PLASMACYTOID DENDRITIC CELLS WITH TLR LIGANDS

Introduction

Plasmacytoid dendritic cells produce copious amounts of type I interferons within 24 hours of viral or bacterial stimulation. What distinguishes pDC as "professional type I Interferon producing cells" is their ability to produce interferon mRNA transcripts within 4 hours following stimulation, with a maximum level of transcripts achieved at 12 hours (Liu, 2005). As specialized cells, they switch their transcriptional machinery after activation primarily to the production of type I interferons. As a subset of dendritic cells, pDC also express pattern recognition receptors (PRR) that recognize conserved pathogen-associated molecular patterns (PAMP), including Toll-like receptors (TLR), protein kinase PKR, and the 2'-5'-oligoadenylate synthase (OAS)/RNase L pathway (Janeway and Medzhitov, 2002). pDC selectively express TLR7 and TLR9, which recognize ssRNA and ssDNA respectively (Fuchsberger *et al*., 2005).

Previous research on pDC stimulation has centered primarily on pDC from the blood, and secondly on lymphoid tissues such as spleen, lymph node and tonsils. A scarcity of studies exists on thymic dendritic cells, and even less on thymic pDC. Subpopulations of thymic dendritic cells can be distinguished based on expression of CD11c, CD14, and CD123; pDC were found to be $CD123^{hi}$, and two myeloid DC subsets

were found to be $CD11c^{+}CD14^{+}$ and $CD11c^{+}CD14^{-}$ (Schmitt *et al.*, 2007). Thymic pDC express lymphoid-specific transcripts, including pre-Tα, Spi-B, and λ-like, maintaining expression of the latter two upon maturation (Bendriss-Vermare *et al*., 2001). Another report used CD11c and B220 (CD45R) to distinguish plasmacytoid and myeloid dendritic cells as pDC express B220 and were found to produce large amounts of IFN-α upon stimulation with TLR9 ligand CpG ODN 2216 (Okada *et al*., 2003). Thymic pDC stimulated with CpG ODN 2216 were comparable in IFN-α production when compared with thymic pDC stimulated with HIV-1, however the combination of both CpG and HIV-1 produced a 4-fold greater IFN-α production than either stimulus alone (Gurney *et al*., 2004).

TLR ligands, including CpG DNA and synthetic ssRNA, allow for in vitro studies without the use of intact bacteria or viruses. Thus, they permit the assessment of activated cell populations without the influence of replicating agents. We exploited the use of synthetic TLR ligands to stimulate thymic pDC in vitro in this study and determined that the cytokine secretion profile of pDC includes a rapid induction of IFN-α, TNF-α, and IL-6.

Materials and Methods

Stimulation of m-PDCA-1^{+} and m-PDCA-1^{-} cells

m-$PDCA1^{+}$ cells and $mPDCA1^{-}$ cells, isolated using MACS as stated above, were plated in duplicate at 2 x 10^{6} cells/ml in 500 µl complete RPMI media (RPMI 1640, 10% FBS, 100 µg/ml streptomycin, 100 units/ml penicillin, 2 mMol L-glutamine, 10 mMol Hepes buffer (pH 7.2), 5.5 µmol 2-mercaptoethanol) in a 24 well flat-bottom plate

(Falcon®, Becton-Dickinson, Franklin Lakes, NJ). Imidazoquinoline compound (CL097) (Invivogen, San Diego, CA) or CpG type A (ODN 1585) (Invivogen, San Diego, CA) were added to stimulate cells at 5 µg/ml and 1 µM, respectfully. Additionally, the m-PDCA^{+} cells received rIL-3 (R & D Systems, Minneapolis, MN) at 10 ng/ml. Cells were cultured for 6 or 24 hours at 37°C with 5% CO_2. After culture, supernatants were collected and stored at -80°C. RNA was extracted from cells using the High Pure RNA Isolation Kit (Roche, Indianapolis, IN) and stored at -80°C.

Quantification of cytokine production

Culture supernatants were assayed for the presence of IFN-α, TNF-α, and IL-6 by enzyme linked immunosorbent assay (ELISA) as specified below.

TNF-α ELISA

The BD OptEIA TNF kit (BD Biosciences, Franklin Lakes, NJ) was used to quantify TNF-α protein in the supernatants. Standards were prepared from a 2000 pg/ml stock solution, serially diluting it resulting in the following concentrations : 1000 pg/ml, 500 pg/ml, 250 pg/ml, 125 pg/ml, 62.5 pg/ml, and 31.3 pg/ml. Equal volumes (50 µl) of ELISA diluent and standard or sample were added to wells of a 96 well plate coated with capture monoclonal antibody specific for mouse TNF-α, and incubated for 2 hours at room temperature. Wells were washed 4 times with 300 µl Wash Buffer (diluted detergent solution) and 100 µl of biotinylated polyclonal anti-mouse TNF-α antibody was added and incubated for 1 hour at room temperature. Wells were washed as previously described, and 100 µl streptavidin-horseradish peroxidase was added to each well for 30

minutes at room temperature. A final wash was completed, and 100 µl of TMB (3,3',5,5'-tetramethylbenzidine) substrate solution was added to each well for 30 minutes at room temperature in the dark. After the last incubation, each well received 50 µl Stop Solution (1M phosphoric acid). The optical density of each sample was read at 450 nm using an ELISA plate reader.

Quantitative PCR for cytokine mRNA

Cytokine transcripts were quantified from stimulated mPDCA1^{+} and mPDCA1^{-} cells using a one-step RT-PCR. Total RNA was extracted using the High Pure Isolation Kit (Roche, Indianapolis, IN) as recommended by the manufacturer according to manufacturer's instructions. A modification was made to the protocol which was a DNase treatment of the samples at 37°C for 30 minutes. Quantitative determination of murine TLR7, TLR9, IFN-α, TNF-α, and IL-6 mRNA was performed using one-step RT fluorescence resonance energy transfer (FRET) PCR in a LightCycler (Roche, Indianapolis, IN). Primers and FRET probes were obtained from Qiagen (Valencia, CA) and are shown in Table 2.

Extraction of total RNA

Total RNA was extracted from the stimulated mPDCA1^{+} and mPDCA1^{-} cells using the High Pure RNA Isolation Kit (Roche Applied Science, Indianapolis, IN) following the manufacturer's instruction. A minor modification of the procedure was employed: DNase treatment of samples was incubated at 37°C for 30 min for the removal of genomic DNA.

Design of primers and probes

Primers and FRET probes were obtained from QIAGEN (Valencia, CA) and are shown in Table 2. In Table 2B, UP indicates the 5'-labeled primer, DN indicates the 3'-labeled primer; BOD and FLU indicate the Bodiby and Carboxyfluorescein probes, respectively. All oligonucleotides were designed by use of the Vector NTI software (InforMax Inc., Frederick, MD) for a calculated T_m of 65° to 70° in the reaction buffer with 190 mMol salt concentration and 100 pM oligonucleotide concentration. Primers and/or probes were designed to bridge exon boundaries when possible, therefore only allowing amplification from, and detection of, cDNA but not genomic DNA (Table 2, Figures 6-7, Figures 9-11). The length of the amplification products was designed to be between 160 and 220 bp. Carboxyfluorescein (6-FAM) probes were 3' labeled and used unpurified as FRET energy donor probes excited by 488 nm light. Bodipy 630/650 and Cy5.5 probes were 5'-labeled, 3'-phosphorylated, HPLC-purified and used as acceptor probes. Fluorescence emitted from Bodipy 630/650 probes served for detection of the target gene mRNAs at 640 nm. In a separate RT-PCR, G6PDH mRNA was detected as a transcript from a housekeeping gene from Cy5.5 probes at 705 nm.

Table 2. Primers and probes used in this study

A. Design

mRNA	TNF-α	IL-6	IFN-α	TLR-7	TLR-9	G3PDH
Amplicon Length	177 bp	210 bp	153 bp	215 bp	183 bp	171 bp
Exons spanned	1-4	1-3	1	1-2	1-2	4-5
Accession #	NM_013693	NM_031168	NM_177361	NM_031178	NM_031178	NM_004285

B. Sequences

TNF-α	UP	GCCACCACGCTCTTCTGTCTACTGAACT
	DN	CTCCACTTGGTGGTTTGCTACGACGT
	BOD	BOD-TTGGGAACTTCTCATCCCTTTGGGGA-P
	FLU	CCATAGAACTGATGAGAGGGAGGCCA-6-FAM
IL-6	UP	GTTCCTCTCTGCAAGAGACTTCCATCCA
	DN	CCATTGCACAACTCTTTTCTCATTTCCAC
	BOD	BOD-ACCAGCATCAGTCCCAAGAAGGCAA-P
	FLU	TTGTGAAGTAGGGAAGGCCGTGGTTGT-6-FAM
IFN-α	UP	CAGCAGCTCAATGACCTGCAAGGCT
	DN	CCAGGCACAGGGGCTGTGTTTCT
	BOD	BOD-TGTGAGGAAATACTTCCACAGGATCACTG-P
	FLU	ACCCAGGAAGACTCCCTGCTGG-6-FAM
TLR-7	UP	CTCCTCCACCAGACCTCTTGATTCCAT
	DN	TGTCAAATGCTTGTCTGTGCAGTCCA

	BOD	BOD-AAAACACCATTTTCAGTTTTCTTTCAAA-P
	FLU	ATTTGTCTCTTCCGTGTCCACATC-6-FAM
TLR-9	UP	GAACATCATTCTCTGCCGCCCAGT
	DN	TGAGGCTTCAGCTCACAGGGTAGGAA
	BOD	BOD-AGAGTCCTTCGACGGAGAACCATG-P
	FLU	CCTGTACCAGGAGGGACAAGGGGTG-6-FAM
G6PDH	UP	AAGCACCTCAACAGCCACATGAATGC
	DN	TCTCCCGAAGGGCTTCTCCACGAT
	Cy5.5	Cy5.5-ATGAGTCAGACAGGCTGGAACCGCAT-P
	FLU	GCAGTCACCAAGAACATTCAAGAGACCTG-6-FAM

Reaction mix and thermal cycling for Real-Time PCR

The PCR buffer was 20 mM Tris-HCl, pH 8.4, 50 mM KCl, 4.5 mM $MgCl_2$, 0.05 % Nonidet P-40, 0.05 % Tween-20, 0.03 % acetylated bovine serum albumin, and 200 μM each dATP, dCTP, dGTP, and 600 μM dUTP. Reactions were performed in glass capillaries with 15 μl of 1.33 x master mixture and 5 μl of sample RNA or standards. Each 20 μl reaction contained 2.0 U Platinum *Taq* DNA polymerase (Invitrogen, Carlsbad, CA), 0.2 U heat-labile uracil-N-glycosylase (Roche Molecular Biochemicals, Indianapolis, IN), and 0.0213 U ThermoScript® reverse transcriptase (Invitrogen, Carlsbad, CA). All primers were used at 1 μM, probes of Bodipy 630/650 and Cy5.5 probes at 0.2 μM, and 6-FAM probes at 0.1 μM. Master mixes were prepared freshly from 10x PCR buffer, 5x oligonucleotide mix, 50x nucleotide mix, and enzymes.

All PCRs were performed on the LightCycler® PCR platform (Roche Molecular Biochemicals, Indianapolis, IN) using LightCycler® Software version 3.5. Thermal cycling was preceded by a 20-minute reverse transcription reaction at 55°C followed by 5 min incubation at 95°C. Thermal cycling consisted of 18 high-stringency step-down cycles followed by 25 relaxed-stringency fluorescence acquisition cycles. The 18 high-stringency step-down thermal cycles were 6 x 15 sec @ 95°C, 60 sec @ 75°C; 9 x 15 sec @ 95°C, 60 sec @ 73°C; 3 x 15 sec @ 95°C, 30 sec @ 71°C, 30 sec @ 72°C. The relaxed-stringency fluorescence acquisition cycling for PCRs consisted of 25 x 15 sec @ 95°C, 8 sec @ 58°C followed by fluorescence acquisition, 30 sec @ 65°C, and 30 sec @ 72°C.

Establishment of quantitative standards

Templates for standard reactions were prepared from RT-PCRs that contained 200 μM dTTP instead of dUTP. PCR products were isolated by 4 % MetaPhor agarose gel electrophoresis, extracted by glass matrix binding and elution (Roche Molecular Biochemicals, Indianapolis, IN), quantified by PicoGreen DNA fluorescence assays (Molecular Probes, Eugene, OR), verified by DNA sequencing, and used at 10^4, 10^3, 10^2, 10, and 0 copies per 5 μl in a background of 100 ng purified pGEM plasmid DNA (Promega, Madison, WI) in $T_{10}E_{0.1}$.

Data analysis

Copy numbers of mRNAs were $\log_2$-transformed to establish normal distribution and the data were analyzed by mean plots ± 95% confidence intervals (CI) in one-way or

factorial ANOVA. Comparisons of means under the assumption of no *a priori* hypothesis were performed by two-tailed Tukey honest significant difference (HSD) test. Differences at $P \leq 0.05$ in the Tukey HSD were considered significant.

Primers and probes

GCCACCACGC TCTTCTGTCT ACTGAACTTC GGGGTGATCG
CGGTGGTGCG AGAAGACAGA TGACTTGAAG CCCCACTAGC

GTCCCCAAAG GGATGAGAAG TTCCCAAATG GCCTCCCTCT
CAGGGGTTTC CCTACTCTTC AAGGGTTTAC CGGAGGGAGA

CATCAGTTCT ATGGCCCAGA CCCTCACACT CAGATCATCT
GTAGTCAAGA TACCGGGTCT GGGAGTGTGA GTCTAGTAGA

TCTCAAAATT CGAGTGACAA GCCTGTAGCC CACGTCGTAG
AGAGTTTTAA GCTCACTGTT CGGACATCGG GTGCAGCATC

CAAACCACCA AGTGGAG
GTTTGGTGGT TCACCTC

Standard curves

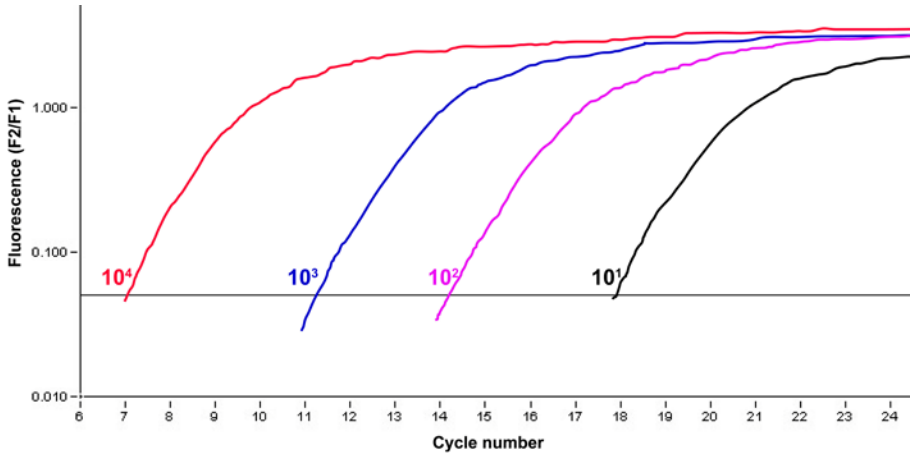

Figure 6. Establishment of quantitative PCR to detect murine TNF-α cDNA. **Upper panel** shows 177 base-pair amplicon bridging exons 1 to 4 of TNF- **α** mRNA. Highlighting indicates primers, red and green indicate probes, and underlined letters indicate the start of a new exon. **Bottom panel** indicates the distribution of quantitative standards of 10^4, 10^3, 10^2, 10^1 copies of TNF-α, and pGEM plasmid DNA reaction as

negative control (resulting in a flat curve under noise band and not showing up under data analysis).

Primers and probes

GTTCCTCTCT GCAAGAGACT TCCATCCAGT TGCCTTCTTG
CAAGGAGAGA CGTTCTCTGA AGGTAGGTCA ACGGAAGAAC

GGACTGATGC TGGTGACAAC CACGGCCTTC CCTACTTCAC
CCTGACTACG ACCACTGTTG GTGCCGGAAG GGATGAAGTG

AAGTCCGGAG AGGAGACTTC ACAGAGGATA CCACTCCCAA
TTCAGGCCTC TCCTCTGAAG TGTCTCCTAT GGTGAGGGTT

CAGACCTGTC TATACCACTT CACAAGTCGG AGGCTTAATT
GTCTGGACAG ATATGGTGAA GTGTTCAGCC TCCGAATTAA

ACACATGTTC TCTGGGAAAT CGTGGAAATG AGAAAAGAGT
TGTGTACAAG AGACCCTTTA GCACCTTTAC TCTTTTCTCA

TGTGCAATGG
ACACGTTACC

Standard curves

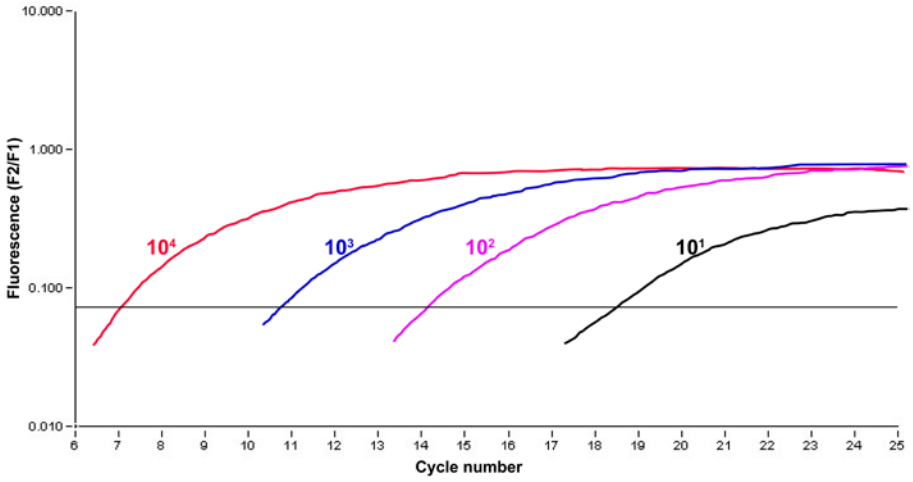

Figure 7. Establishment of quantitative PCR to detect murine IL-6 cDNA. **Upper panel** shows 210 base-pair amplicon bridging exons 1 to 3 of IL-6 mRNA. Highlighting indicates primers, red and green indicate probes, and underlined letters indicate the start of a new exon. **Bottom panel** indicates the distribution of quantitative standards of 10^4,

10^3, 10^2, 10^1 copies of IL-6, and pGEM plasmid DNA reaction as negative control (resulting in a flat curve under noise band and not showing up under data analysis).

Primers and probes

Standard curves

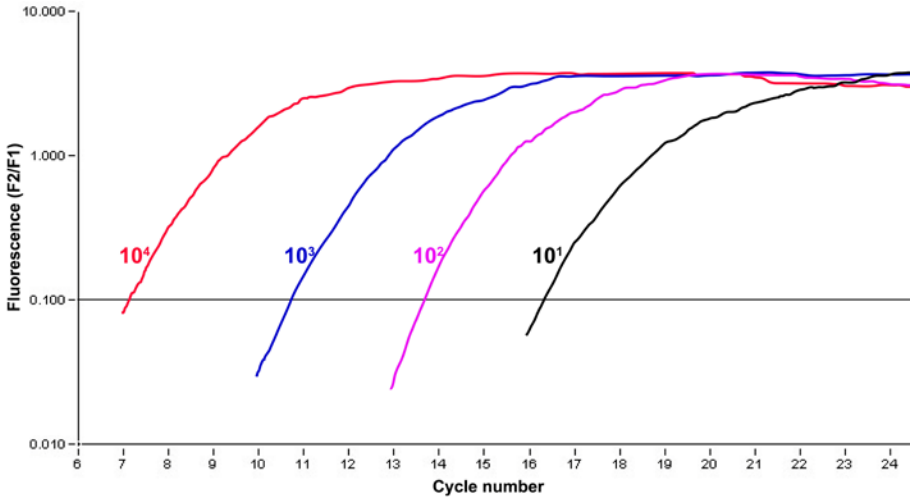

Figure 8. Establishment of quantitative PCR to detect murine IFN-α cDNA. **Upper panel** shows 153 base-pair amplicon for IFN-α mRNA. Highlighting indicates primers, red and green indicate probes, and underlined letters indicate the start of a new exon. This gene has a single exon in murine species. **Bottom panel** indicates the distribution of quantitative standards of 10^4, 10^3, 10^2, 10^1 copies of IFN-α, and pGEM plasmid DNA

reaction as negative control (resulting in a flat curve under noise band and not showing up under data analysis).

Primers and probes

CTCCTCCACC AGACCTCTTG ATTCCATTTT GAAAGAAAAC
GAGGAGGTGG TCTGGAGAAC TAAGGTAAAA CTTTCTTTTG

TGAAAATGGT GTTTTCGATG TGGACACGGA AGAGACAAAT
ACTTTTACCA CAAAAGCTAC ACCTGTGCCT TCTCTGTTTA

TTTGATCTTT TTAAATATGC TCTTAGTTTC TAGAGTCTTT
AAACTAGAAA AATTTATACG AGAATCAAAG ATCTCAGAAA

GGGTTTCGAT GGTTTCCTAA AACTCTACCT TGTGAAGTTA
CCCAAAGCTA CCAAAGGATT TTGAGATGGA ACACTTCAAT

AAGTAAATAT CCCAGAGGCC CATGTGATCG TGGACTGCAC
TTCATTTATA GGGTCTCCGG GTACACTAGC ACCTGACGTG

AGACAAGCAT TTGACA
TCTGTTCGTA AACTGT

Standard curves

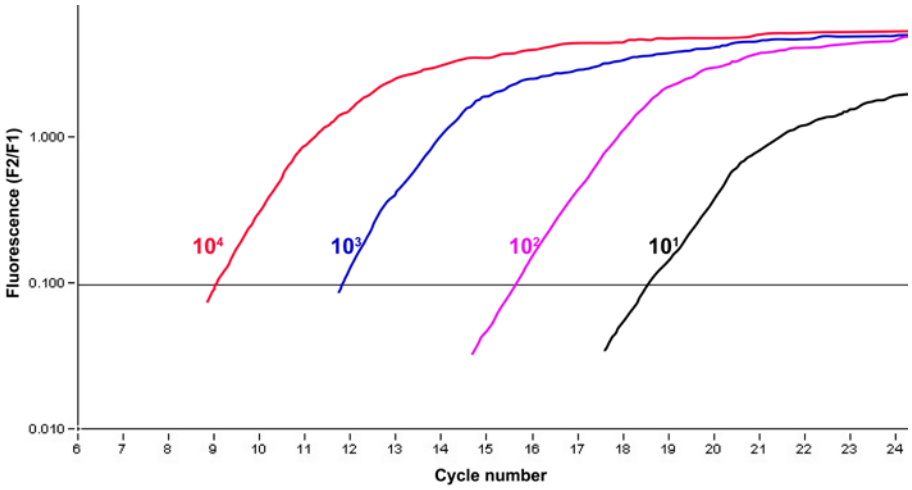

Figure 9. Establishment of quantitative PCR to detect murine TLR-7 cDNA. **Upper panel** shows 215 base-pair amplicon bridging exons 1 to 2 of TLR-7 mRNA. Highlighting indicates primers, red and green indicate probes, and underlined letters indicate the start of a new exon. **Bottom panel** indicates the distribution of quantitative standards of 10^4, 10^3, 10^2, 10^1 copies of TLR7, and pGEM plasmid DNA reaction as

negative control (resulting in a flat curve under noise band and not showing up under data analysis).

Primers and probes

GAACATCATT CTCTGCCGCC CAGTTTGTCA GAGGGAGCCT
CTTGTAGTAA GAGACGGCGG GTCAAACAGT CTCCCTCGGA

CGGGAGAATC CTCCATCTCC CAACATGGTT CTCCGTCGAA
GCCCTCTTAG GAGGTAGAGG GTTGTACCAA GAGGCAGCTT

GGACTCTGCA CCCCTTGTCC CTCCTGGTAC AGGCTGCAGT
CCTGAGACGT GGGGAACAGG GAGGACCATG TCCGACGTCA

GCTGGCTGAG ACTCTGGCCC TGGGTACCCT GCCTGCCTTC
CGACCGACTC TGAGACCGGG ACCCATGGGA CGGACGGAAG

CTACCCTGTG AGCTGAAGCC TCA
GATGGGACAC TCGACTTCGG AGT

Standard curves

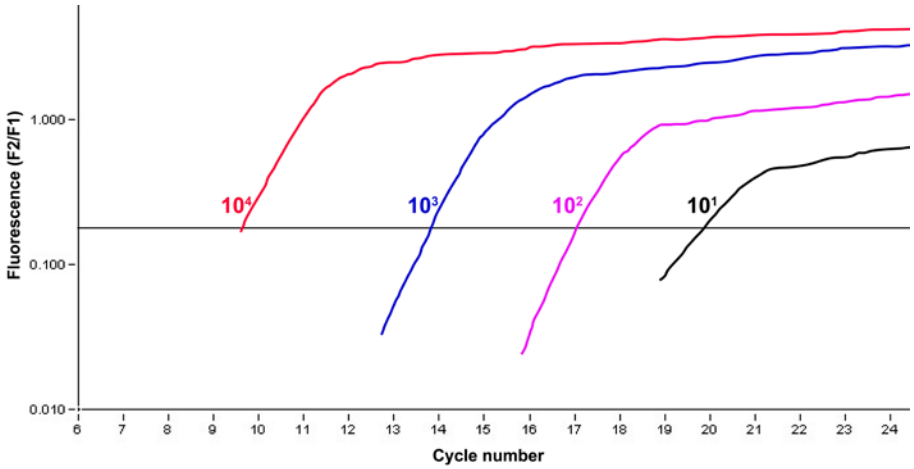

Figure 10. Establishment of quantitative PCR to detect murine TLR-9 cDNA. **Upper panel** shows 183 base-pair amplicon bridging exons 1 to 2 of TLR-9 mRNA. Highlighting indicates primers, red and green indicate probes, and underlined letters indicate the start of a new exon. **Bottom panel** indicates the distribution of quantitative standards of 10^4, 10^3, 10^2, 10^1 copies of TLR9, and pGEM plasmid DNA reaction as

negative control (resulting in a flat curve under noise band and not showing up under data analysis).

Primers and probes

AAGCACCTCA ACAGCCACAT GAATGCCCTG CACCAGGGGA
TTCGTGGAGT TGTCGGTGTA CTTACGGGAC GTGGTCCCCT

TGCAGGCCAA CCGTCTATTC TACCTGGCCT TGCCCCCCAC
ACGTCCGGTT GGCAGATAAG ATGGACCGGA ACGGGGGGTG

AGTCTATGAA GCAGTCACCA AGAACATTCA AGAGACCTGC
TCAGATACTT CGTCAGTGGT TCTTGTAAGT TCTCTGGACG

ATGAGTCAGA CAGGCTGGAA CCGCATCATC GTGGAGAAGC
TACTCAGTCT GTCCGACCTT GGCGTAGTAG CACCTCTTCG

CCTTCGGGAG A
GGAAGCCCTC T

Standard curves

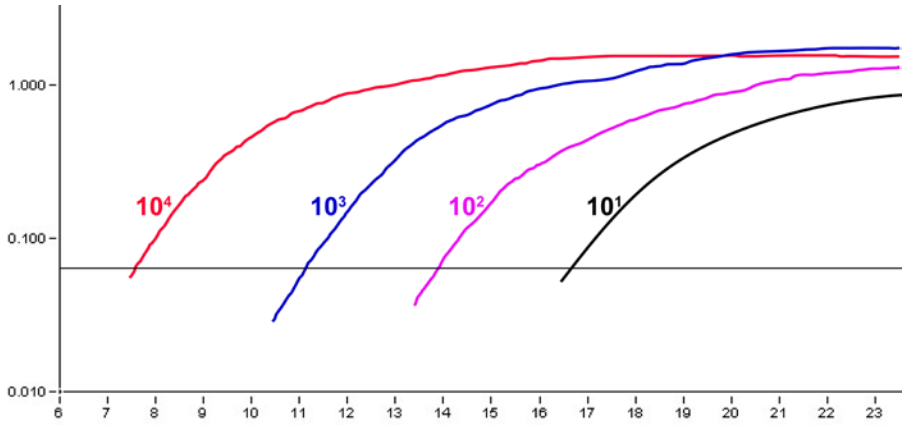

Figure 11. Establishment of quantitative PCR to detect murine G6PDH cDNA. **Upper panel** shows 171 base-pair amplicon bridging exons 4 to 5 of G6PDH mRNA. Highlighting indicates primers, red and green indicate probes, and underlined letters indicate the start of a new exon. **Bottom panel** indicates the distribution of quantitative standards of 10^4, 10^3, 10^2, 10^1 copies of G6PDH, and pGEM plasmid DNA reaction as

negative control (resulting in a flat curve under noise band and not showing up under data analysis).

Results

Stimulation with TLR7 and TLR9 ligands

Murine thymic pDC were successfully stimulated in vitro with TLR7 and TLR9 ligands. Stimulated m-PDCA-1$^+$ cells produced large amounts of TNF-α protein compared with stimulated m-PDCA-1$^-$ cells (Fig. 12). m-PDCA-1$^+$ cells stimulated with TLR7 and TLR9 ligands produced greater quantities of TNF-α protein compared with those unstimulated and negative control supernatant (Fig. 12). Interestingly, m-PDCA-1$^+$ cells stimulated with TLR9 ligand alone secreted a higher amount of TNF-α than those stimulated with both TLR7 and TLR9 ligands together (Fig. 12). This could be because both TLR7 and TLR9 use the same signaling pathway, and are both dependent on the adaptor protein MyD88 (Moynagh, 2005).

Quantitative RT-PCR was used to measure cytokine transcripts of stimulated and unstimulated m-PDCA-1$^+$ cells for TNF-α, IL-6, IFN-α, and transcripts of the housekeeping gene G6PDH. Total RNA was extracted from stimulated and unstimulated cells, treated with DNase, and cDNA was synthesized in the presence of reverse transcriptase. Stimulated m-PDCA-1$^+$ cells had higher expression of IL-6 transcripts compared to unstimulated m-PDCA-1$^+$ cells, although transcripts of the housekeeping gene G6PDH remained alike (Fig. 13). IL-6 transcripts from m-PDCA-1$^+$ cells peaked at 6 hours post stimulation, but levels remained high even at 24 hours post stimulation (Fig. 15). Additionally, levels of TNF-α transcripts peaked at 6 hours post activation and were

still detectable at 24 hours post stimulation (Fig. 16). We were unable to compare IFN-α mRNA levels in stimulated and unstimulated m-PDCA-1^{+} cells due to inability to detect IFN-α transcripts over the background of intronless IFN α genes in contaminating genomic DNA (Fig. 14). However, published reports have indicated that type I IFN mRNA can be detected at 4 hours post stimulation resulting in peak mRNA at 12 hours (Ito *et al*., 2006).

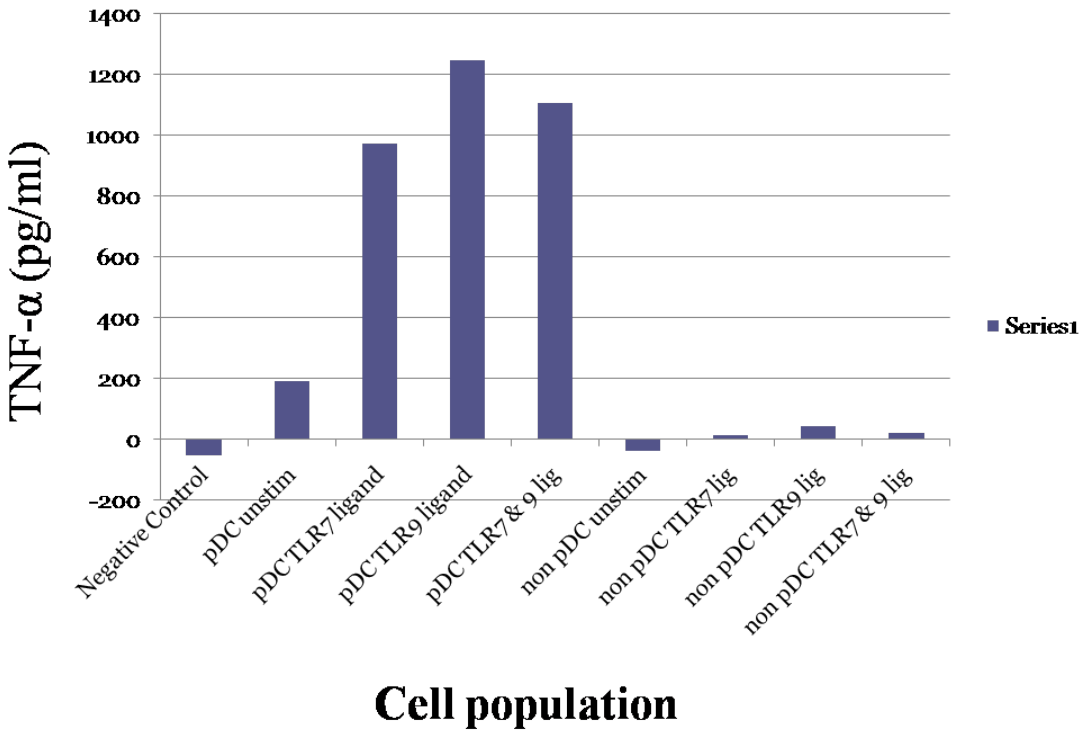

Figure 12. Quantification of TNF-α protein from supernatants of m-PDCA-1^{+} and m-PDCA-1^{-} cells using ELISA. pDC produced abundant TNF-α when compared to non-pDC cells after stimulation with TLR7 ligand, TLR9 ligand, or the combination of both. Supernatant from feline CD4^{+} T cells was used as a negative control. Results represent a single experiment; therefore, no statistical analysis was performed.

transcript (IL-6)

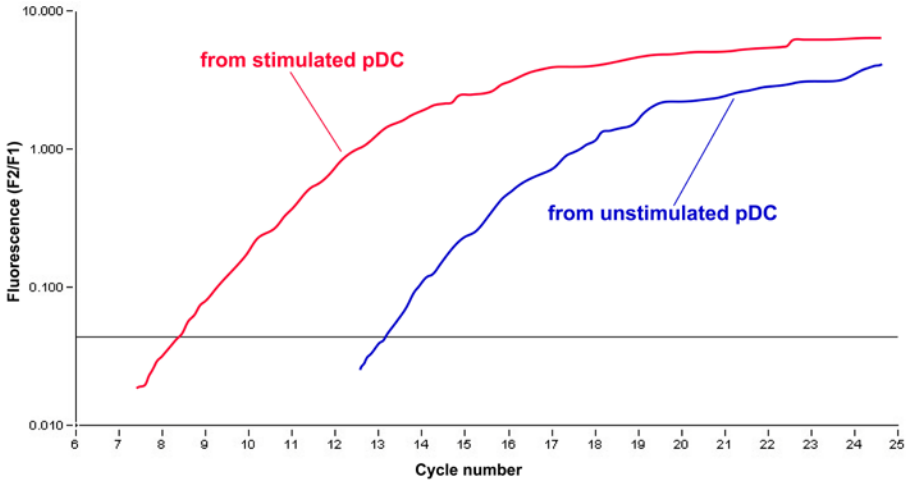

housekeeping gene (G6PDH)

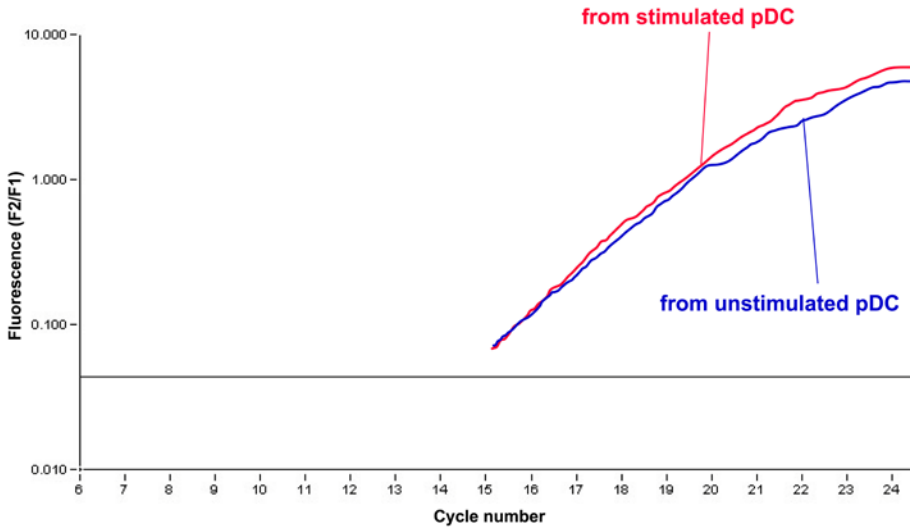

Figure 13. Quantitative detection of murine IL-6 transcripts from stimulated and un-stimulated pDC. Stimulated pDC showed a higher expressional level of IL-6 than that of unstimulated pDC (**upper panel**) while the transcript levels of G6PDH as housekeeping gene were similar between stimulated pDC and unstimulated pDC (**bottom panel**).

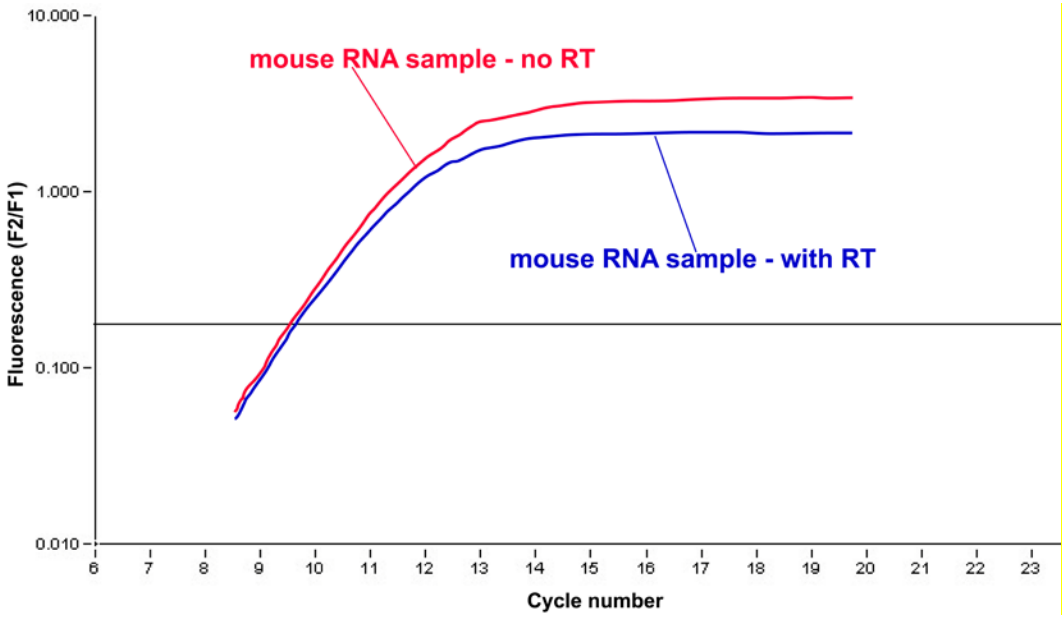

Figure 14. RT-PCR designed to quantify murine IFN- α mRNA within a single exon. There was not an appreciable difference between amplification levels with or without the addition of reverse transcriptase (RT), indicating that the assay was not a valid measurement of mRNA expression. Similar results were obtained despite repeated attempts to remove genomic DNA through a variety of methods, including extended DNAse treatment and oligo dT selection of poly A RNA.

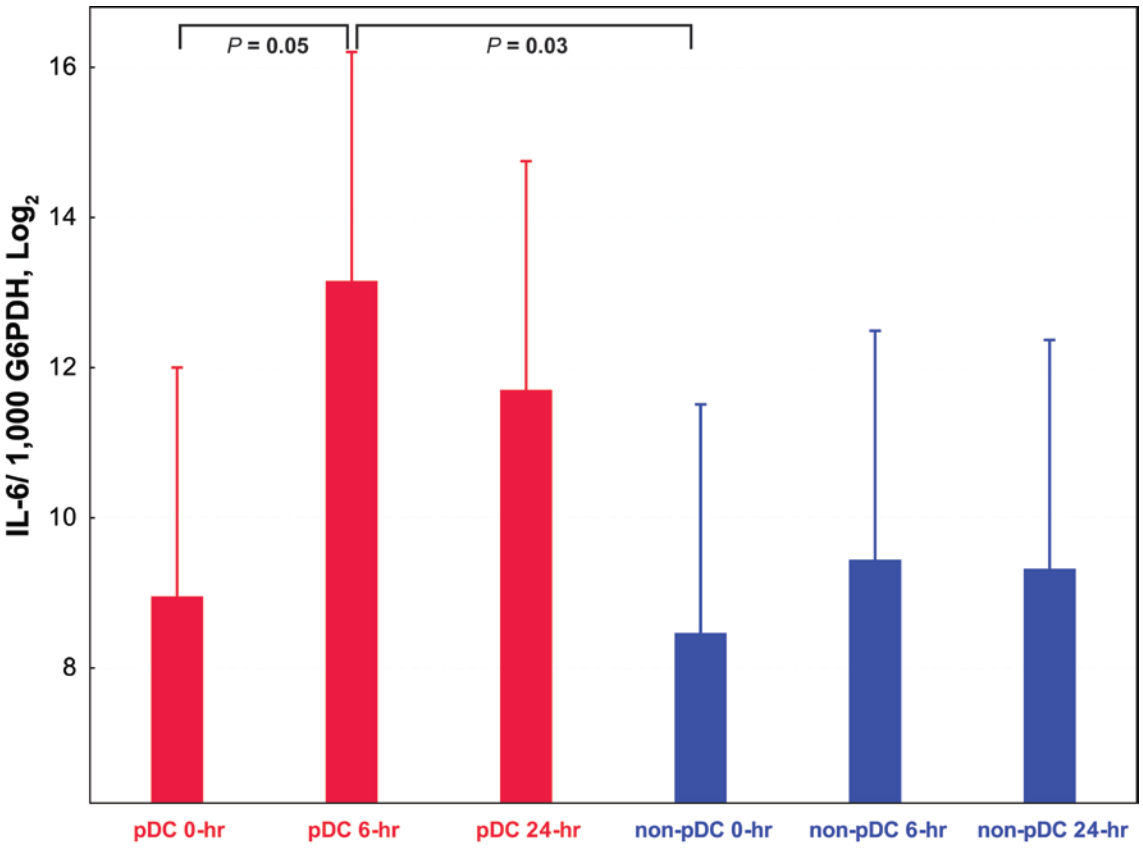

Figure 15. Stimulated pDC showed significantly up-regulated levels of IL-6 transcripts. Data were log2 transformed to create a normal distribution and analyzed by one-way ANOVA. Comparisons of means were performed by the two-tailed Tukey honest significant differences (HSD) test. Error bar, ±95% confidence interval. n = 4 repeats / treatment. pDC cells, six-hour after TLR9 treatment (1 μM), showed significantly increased IL-6 transcripts ($2^{13.15}$±$2^{3.59}$; 24,670±20,345) than pDC cells not receiving treatment ($2^{8.95}$±$2^{0.64}$; 538±280), and non-pDC cells not receiving treatment ($2^{8.46}$±$2^{3.32}$; 4,092±8,832)

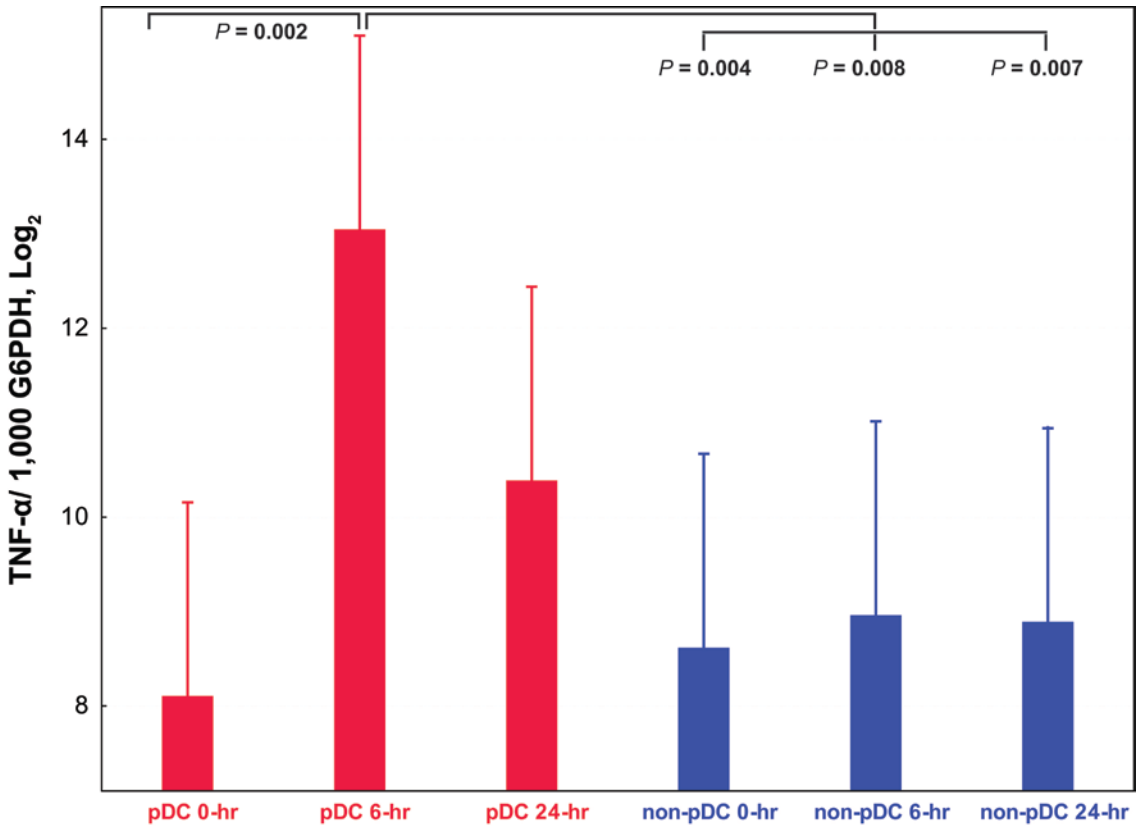

Figure 16. Stimulated pDC showed significantly up-regulated levels of TNF-α transcripts. Data were log2 transformed to create a normal distribution and analyzed by one-way ANOVA. Comparisons of means were performed by the two-tailed Tukey honest significant differences (HSD) test. Error bar, ±95% confidence interval. n = 4 repeats / treatment. pDC cells, six-hour after TLR9 treatment (1 µM), showed significantly increased TNF-α transcripts ($2^{13.04}\pm2^{3.11}$; 66,669±145,867) than pDC cells not receiving treatment ($2^{8.10}\pm2^{1.72}$; 613±1,049), and non-pDC cells not receiving treatment ($2^{8.61}\pm2^{2.60}$; 1,923±3,946), and 6 hours ($2^{8.96}\pm2^{2.42}$; 1,373±1,971) and 24 hours ($2^{9.88}\pm2^{1.21}$; 644±576) after receiving treatment.

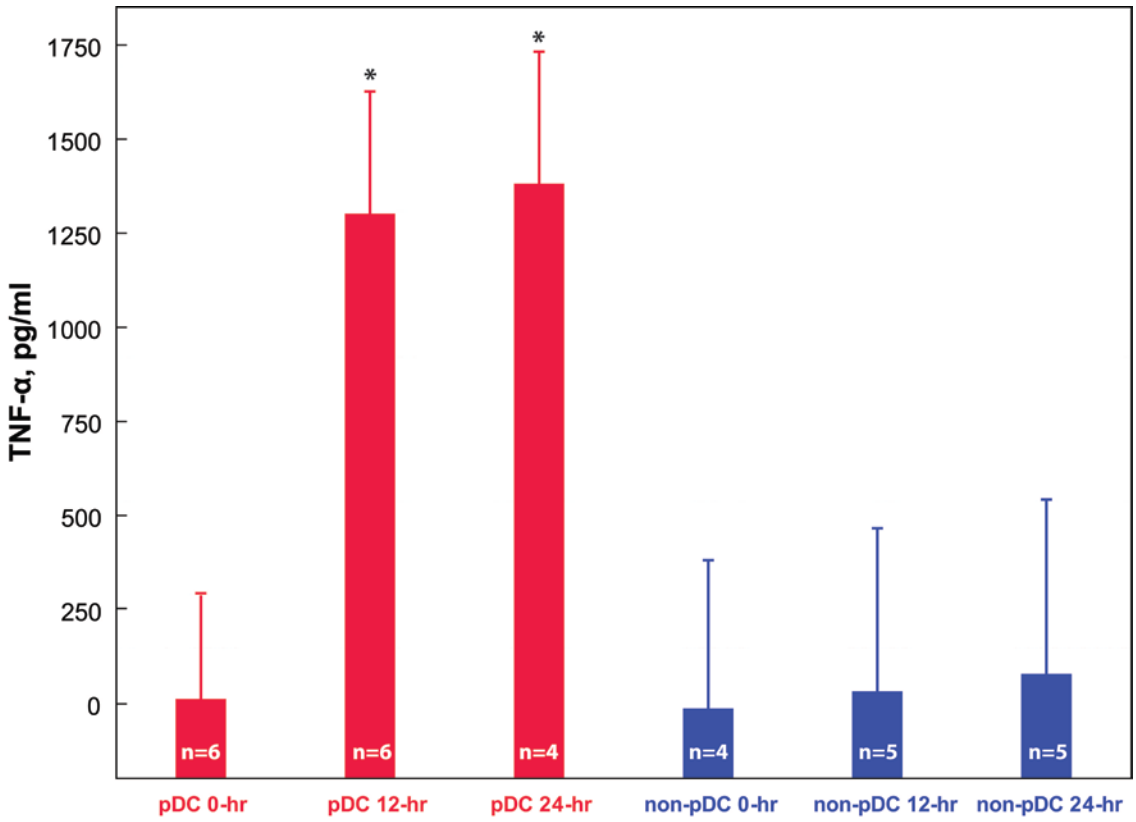

Figure 17. Stimulated pDC showed significantly up-regulated levels of TNF-α protein compared to unstimulated pDC and stimulated non-pDC cells. Levels of TNF-α in supernatants were measured in triplicate and then analyzed by one-way ANOVA. Comparisons of means were performed by the two-tailed Tukey honest significant differences (HSD) test. Error bar, ±95% confidence interval. Asterisks (*) indicate significant differences ($p<0.05$).

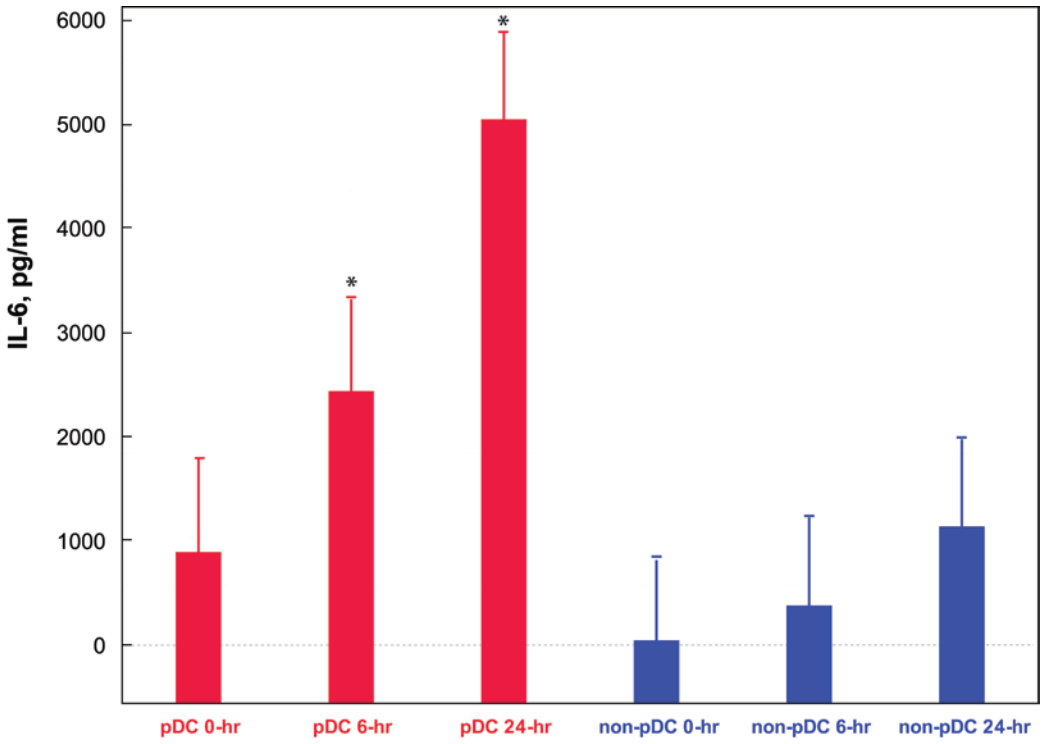

Figure 18. Stimulated pDC showed significantly up-regulated levels of IL-6 protein compared to unstimulated pDC and stimulated non-pDC cells. Levels of IL-6 in supernatants were measured in triplicate and then analyzed by one-way ANOVA. Comparisons of means were performed by the two-tailed Tukey honest significant differences (HSD) test. Error bar, ±95% confidence interval. Asterisks (*) indicate significant differences ($p<0.05$).

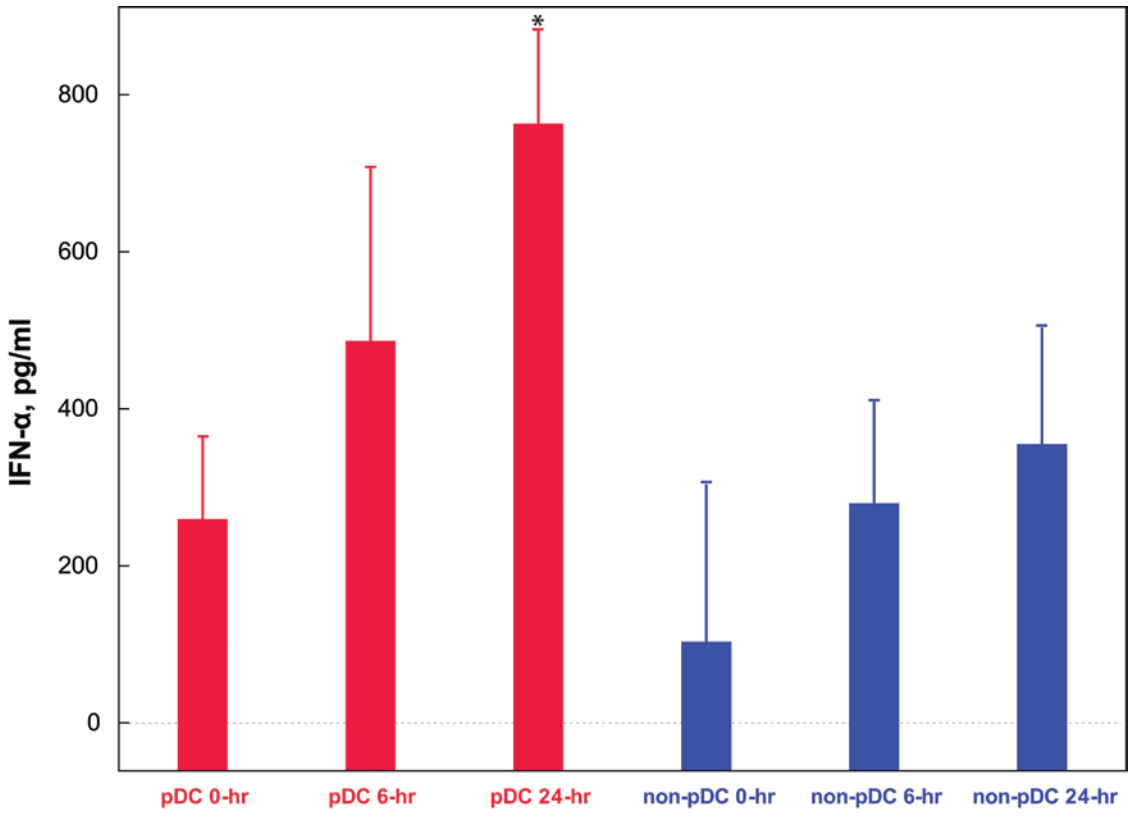

Figure 19. Stimulated pDC showed significantly up-regulated levels of IFN-α protein compared to unstimulated pDC and stimulated non-pDC cells. Levels of IFN-α in supernatants were measured in triplicate and then analyzed by one-way ANOVA. Comparisons of means were performed by the two-tailed Tukey honest significant differences (HSD) test. Error bar, ±95% confidence interval. Asterisks (*) indicate significant differences ($p<0.05$).

Discussion

Results of this study showed that pDC, enriched from the murine thymus, produced higher levels of TNF-α and IL-6 transcripts and TNF-α, IL-6, and IFN-α

protein upon stimulation with TLR ligand compared to non-pDC cells. A valid RT-PCR assay for IFN-α was not developed. The levels of protein seen here are comparable to levels of proinflammatory cytokines of stimulated pDC in published reports (Veckman and Julkenen, 2008). Veckman *et al*. (2008) found stimulated pDC produced 0.15 ng/ml TNF-α, 0.2 ng/ml IL-6, and 2 ng/ml IFN-α in cell supernatants 24 hours after stimulation with influenza A virus. High levels of IFN-α in our non-pDC fraction indicate the existence of contamination of the non-pDC cell fraction with a cell population (likely pDC) that expressed high levels of IFN-α. As TLR9 ligand was used to stimulate cells in both the non-pDC and pDC fractions of cells, only cells expressing TLR9 would be activated. Cells that are TLR9 positive include pDC and B cells, and B cells would be found in minimal numbers in the thymus. Thus, we conclude that a small, but functionally significant number of pDC contaminated the non-pDC fraction of cells.

For reverse-transcription PCR, we routinely design primers and probes to overlap two or more exons so that RT-PCR would only amplify the mRNA target, not genomic DNA. However, this strategy was not useful for murine IFN-α because this gene contains only a single exon. Therefore, we tried to remove genomic DNA by treating the total nucleic acids with DNase and by selecting the mRNA with oligo-dT coated beads. Despite these attempts, we were not able to completely remove genomic DNA as seen in Figure 14. Similar amplification levels were seen for the sample with and without reverse transcriptase. The use of multiple DNase treatments became too harsh for mRNA and accordingly no RT-PCR amplification was seen (data not shown). In spite of the strategy to test mRNA samples in the reaction with and without reverse transcriptase, we have to accept at this time that we are not able to amplify INF-α mRNA copies with

ensured specificity. This finding underscores the importance of careful design and systematic analysis of appropriate controls to validate methods for the quantification of mRNA targets, particularly those with single or two exons.

pDC isolated from the murine thymus were stimulated and activated to produce pro-inflammatory cytokines (TNF-α, IL-6, and IFN-α), both in gene transcripts (in the case of the former two) and protein found in the supernatant. It is evident, however, based on the cytokine levels of unstimulated populations that the enrichment and isolation procedures contributed to their activation, even in the absence of other exogenous stimuli. Potentially, ligation of m-PDCA-1 by the sorting monoclonal antibody during the enrichment process resulted in stimulation of pDC. Other enrichment procedures will need to be developed that have a reduced effect on the stimulation of pDC.

CHAPTER 4

EFFECT OF STIMULATED THYMIC pDC ON THYMUS ORGAN CULTURE

Introduction

T cell development involves a series of complex events with distinct selection processes to generate a T cell repertoire that is MHC-restricted and self-tolerant. The study of T cell differentiation in vitro offers advantages over in vivo studies, including the isolation of distinct selection events through monoclonal antibody blockade, addition of recombinant cytokines, and avoidance of toxicity associated with administered reagents. A few in vitro model systems are currently in use to study the cellular interactions of thymopoiesis such as the culture of entire or reaggregated mouse fetal thymic lobes and the culture of hematopoietic progenitors on a stromal cell line (Ramsdell *et al*., 2006).

Thymus organ culture (TOC) is an in vitro system of culturing explanted murine fetal thymuses to study the phenotypic and functional changes of developing thymocytes. Thymus grafts are positioned at the interface of air and medium, to maximize the exchange of gases and nutrients. The isolation of ex vivo T cell development allows for manipulation of precise conditions without the confounding physiologic influences. TOC systems are used to study central T-cell tolerance and the role of peptides in the

differentiation of T cells (Ashton-Rickardt, 2007) and have been used to research replication and pathogenesis of HIV-1 in the thymus (Meissner *et al*., 2003).

Very little research has studied the effect of stimulated thymic pDC on T cell development. One study showed stimulated pDC, generated in vitro using thymic precursor cells cocultured with the OP9-Jag1 cell line, had a deleterious effect on early T cell development (Schmidlin *et al*., 2006). Baron *et al*. (2008) demonstrated the addition of TLR ligands or IFN-α treatment to fetal thymus organ culture resulted in a blockade to the early steps of thymopoiesis. To our knowledge, there exist no reports of effects of stimulated pDC on thymopoiesis using freshly sorted pDC from thymus tissue. The current study reports the effect of pDC, after TLR ligation on developing thymocytes in TOC.

Materials and Methods

Thymus organ culture

For each experiment, the intact uteri were retrieved from two pregnant ICR mice (20 days of gestation based on observation of vaginal plugging) immediately after euthanasia by cervical dislocation. In some experiments, neonatal mice were obtained within 12 hours of birth. The fetuses or neonates were placed on moist sterile gauze under a dissecting microscope (6X magnification, Leica MZ6, Wetzlar, Germany). After the heads were removed, the chest cavity was opened up with shallow incisions into the sternum. The thymic lobes were located in the chest cavity and teased away from nearby tissue, and then grasped using iris forceps and placed in sterile PBS in a petri dish on ice.

Gelfoam sponges (Upjohn, Kalamazoo, MI) were cut with sterile surgical scissors into 20 mm x 20 mm squares and placed in a 12 well plate. 1.5 or 2 ml of TOC media (DMEM-10, 10% FBS, 2 mM L-glutamine, 100 U/ml Penicillin, 100 µg/ml Streptomycin, 50 µM 2-mercaptoethanol) was added to each well to saturate Gelfoam square sponges. A sterile Nucleopore polycarbonate membrane (Whatman, Florham Park, NJ) was added to each Gelfoam sponge (Fig. 20). Four or five thymic lobes were transferred to each Nucleopore membrane using iris forceps. One well received only TOC media, a second received 70% conditioned media from stimulated pDC, a third well received 70% conditioned media from unstimulated pDC, and a fourth well received TLR9 ligand ODN1585 at 1 µM in TOC media. Thymuses were cultured for four days at 37°C with 5% CO_2. Two thymuses were reserved for initial phenotypic analysis and a viable cell count was performed using the trypan blue exclusion test.

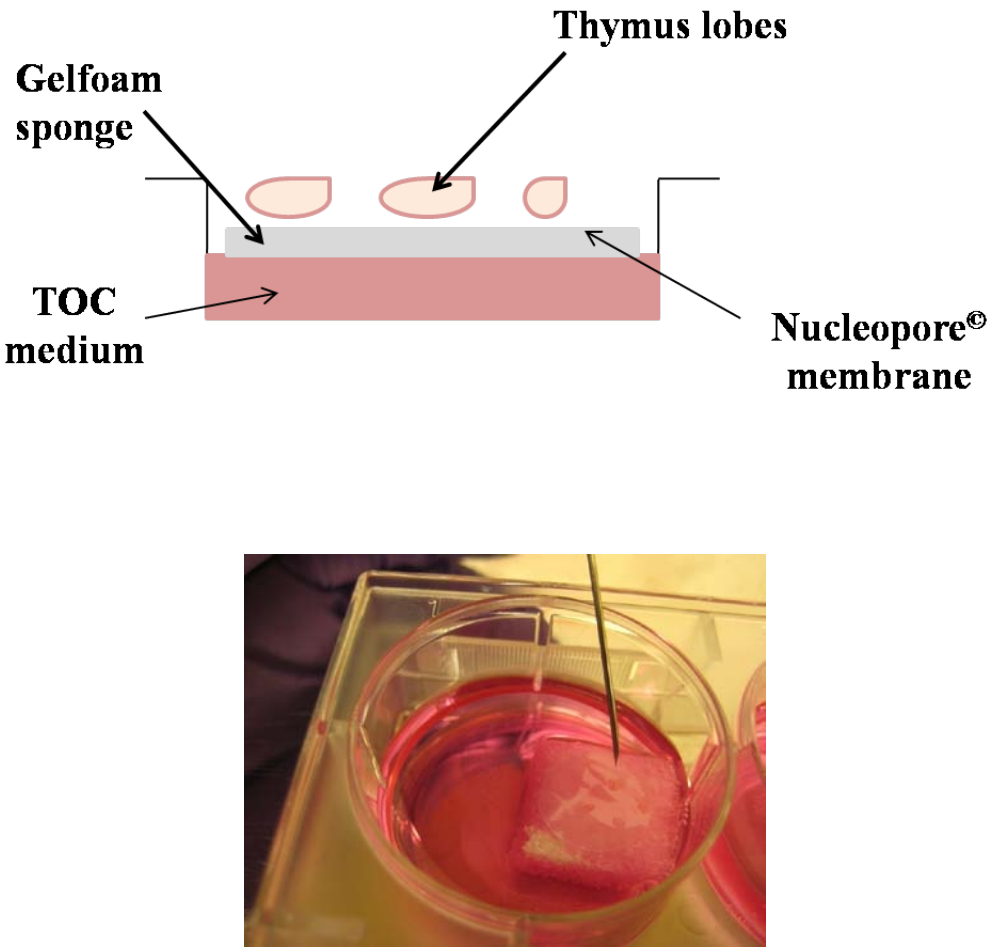

Figure 20. Murine thymus organ culture model **Upper panel:** Thymus organ culture set-up. **Lower panel:** Photograph of thymus organ culture experiment; showing Gelfoam square in TOC medium with Nucleopore membrane. Needle is pointing to thymus lobes dotting the surface of the membrane.

Flow cytometric analysis of thymopoiesis

Thymic lobes were removed from the Nucleopore membranes at the end of the four-day incubation period using sterile iris forceps and placed in 500 µl sterile PBS. A cell suspension was prepared through teasing the thymic lobes apart with two 25-gauge

needles under the dissecting microscope. Cell suspensions were filtered through a 100 µm Falcon cell strainer (BD Biosciences, Franklin Lakes, NJ) and a cell count was performed on each group. Cells were stained in 1.5 ml Eppendorf tubes with monoclonal antibodies recognizing rat IgG2b-FITC (AbD Serotec, Raleigh, NC), CD4-Alexa700 (0.2 mg/ml) (eBioscience, San Diego, CA), CD8α-FITC (0.5 mg/ml) (eBioscience, San Diego, CA), and incubated for 30 minutes in the dark on ice. Cells were washed twice with the addition of 700 µl flow buffer (1X PBS, 2% FBS) and then centrifuged at 300 *g* for 5 minutes at 4°C. Thymocytes were resuspended in 500 µl flow buffer and analyzed on a MoFlo cytometer (Dako Cytomation) with Summit software.

Neutralization Assay

Thymus organ culture was set up as previously described. Five thymic lobes were transferred to each Nucleopore membrane, on a Gelfoam square in 560 µl TOC media. Blocking antibodies used were anti-murine IFN-α (10µg/ml) (PBL Interferon Source, Piscataway, NJ), anti-murine TNF-α (10µg/ml) (BioVision, Mountain View, CA), and anti-murine IL-6 (1µg/ml) (BioVision, Mountain View, CA). Antibodies were added to supernatant, incubated for 2 hours at 37°C and then transferred to appropriate TOC wells. Three wells each received supernatants previously incubated with blocking antibodies IFN-α, TNF-α and IL-6. A final well received supernatant incubated with all 3 antibodies concurrently. Controls included one well that received only TOC media, and a second well that received 70% conditioned media from stimulated pDC. TOC were cultured for four days at 37°C with 5% CO_2. Two thymuses were reserved for initial phenotypic analysis. Following incubation, thymic lobes were removed from each well and a single

cell suspension was prepared as described above. Thymocytes were stained using antibodies recognizing rat IgG2b-FITC, CD4-Alexa700, CD8α-FITC as previously described and analyzed on a MoFlo cytometer (Dako Cytomation) with Summit software.

Results

Phenotypic analysis

In this study, we tested the hypothesis that thymic pDC, activated through TLR ligation, can alter the phenotype of developing thymocytes. Thymus organ cultures were successfully maintained for 4 days and subsequently each treatment group was analyzed by flow cytometry to identify specific phenotypic changes. Fresh thymocytes were analyzed prior to TOC to establish an initial phenotypic profile of developing thymocytes. The scatterplot of these thymocytes revealed a homogeneous population of small and nongranular cells, typical of thymocytes (Fig. 21A). Fresh thymocytes were predominantly (74%) a double positive ($CD4^+CD8^+$) phenotype , 6% were CD4 single positive ($CD4^+CD8^-$), 3% were CD8 single positive ($CD4^-CD8^+$), and 17% were double negative ($CD4^-CD8^-$) (Fig 21B). Thymocytes cultured in TOC after 4 days were larger and more granular (Fig. 21C.) These thymocytes retained a primarily double positive (CD4+CD8+) phenotype at 68.9%, while single positive CD4 cells increased to 9.2% and single positive CD8 cells increased to 5.1%, and 16.7 % of cells were double negative (Fig. 21D). Thymocytes from TOC that received 70% conditioned media from stimulated pDC had a lower percentage (55%) of double positive cells, and higher percentages of both single positive populations and double negative thymocytes (Fig. 21E). Thymocytes from TOC that received 70% conditioned media from unstimulated

pDC resembled control TOC in phenotype with a higher percentage of double positive (64.5%), and lower percentages of single positive CD4 and CD8 cells (Fig. 21F.) The phenotype of thymocytes in TOC that received TLR9 ligand ODN1585 was 62% double positive (CD4+CD8+), 8.8% CD4 single positive (CD4+CD8-), 10.5% CD8 single positive (CD4-CD8+), and 18.4% double negative (CD4-CD8-) (Fig 21G).

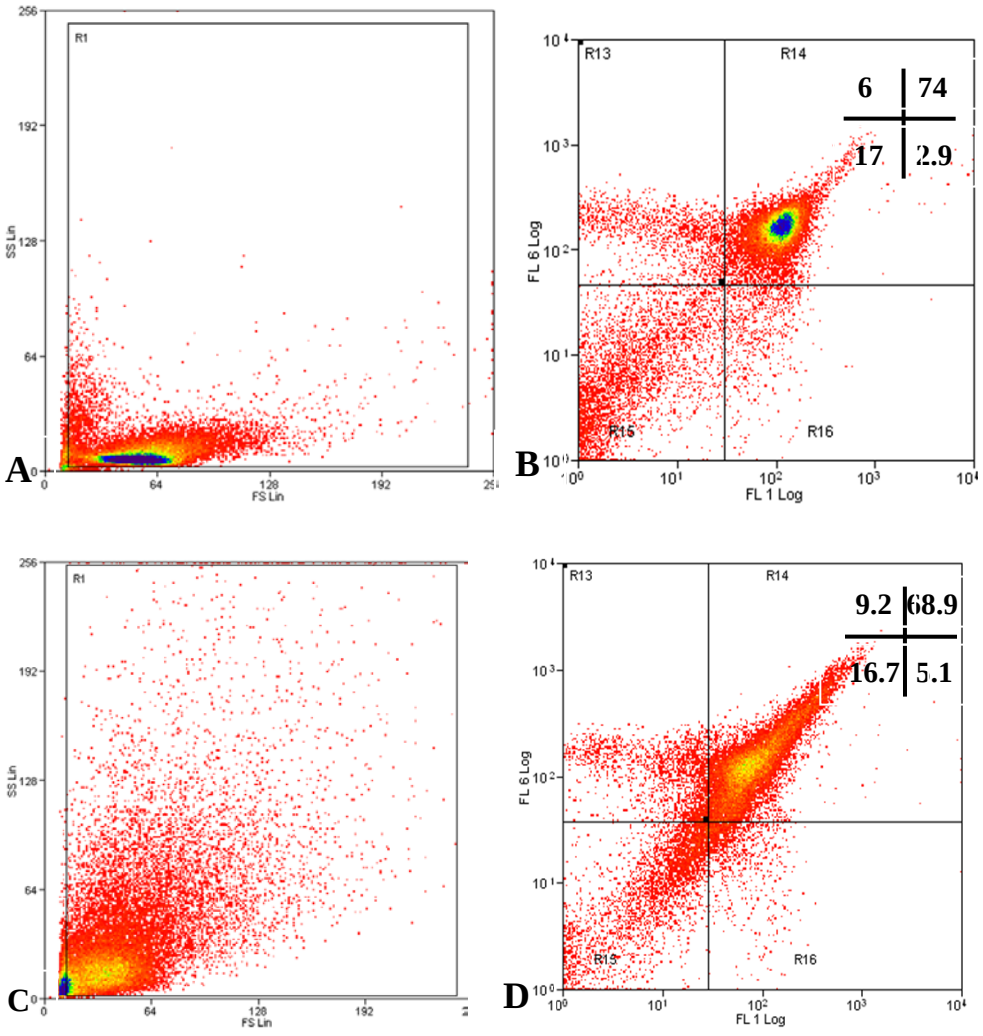

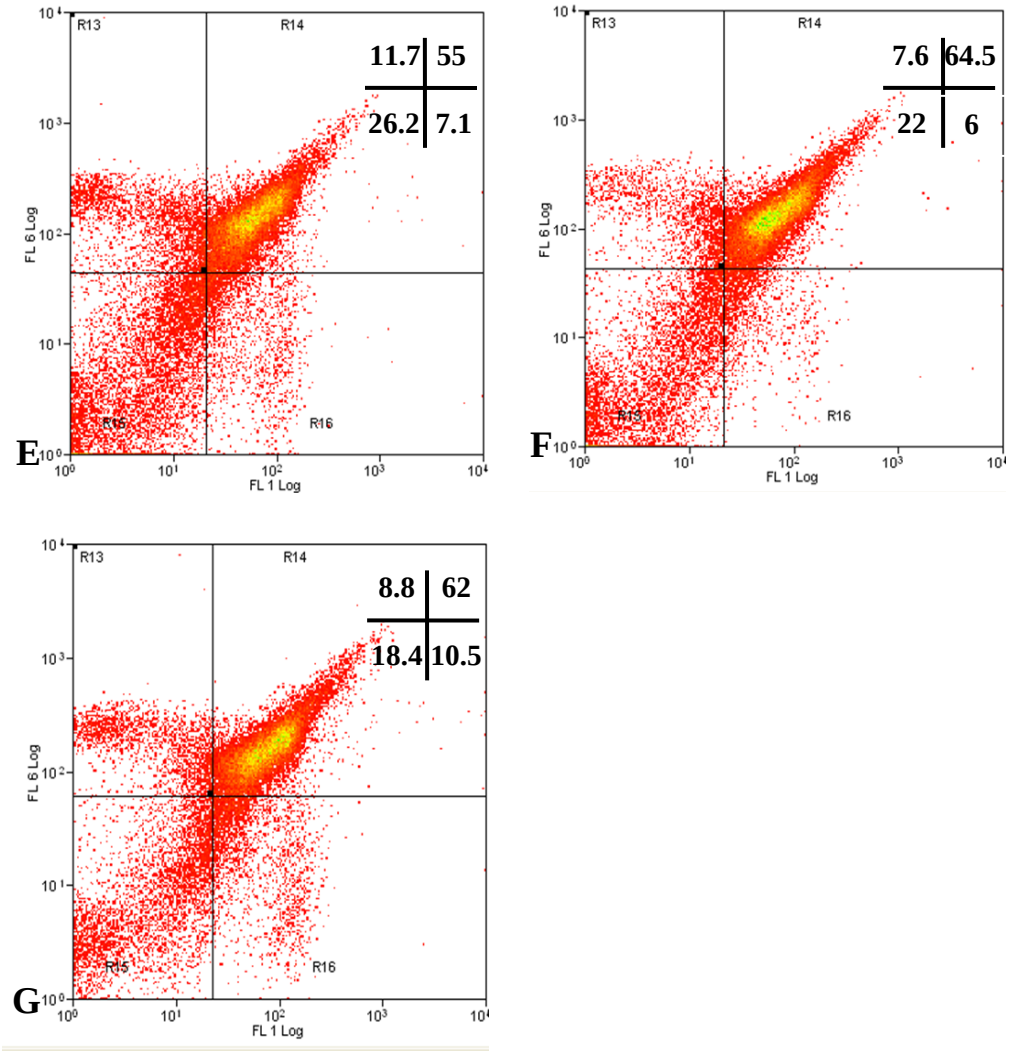

Figure 21. Flow cytometric analysis of fresh thymocytes, control and treatment groups of TOC. Cells were stained with CD8α-FITC (FL1) and CD4-Alexa 647 (FL6) **A**. Scatterplot of fresh thymocytes **B**. Fresh thymocytes **C**. Scatterplot of control thymocytes in TOC after 4 days **D.** Control thymocytes in TOC after 4 days **E.** TOC group received 70% conditioned media from stimulated pDC **F.** TOC group received 70% conditioned media from unstimulated pDC **G.** TOC received TLR9 ligand ODN 1585

Thymocytes were recovered after the designated incubation period, and their phenotype was determined using CD8α-FITC and CD4-Alexa647 or -Alexa700 to evaluate the effect of conditioned media from stimulated pDC, unstimulated pDC, and addition of TLR9 ligand. The percentage of double positive thymocytes ($CD4^+CD8^+$) in TOC after 4 days was not significantly different than double positive thymocytes in a fresh thymus (Fig.22). Furthermore, treatment with media of stimulated pDC, unstimulated pDC, or TLR9 ligand had no significant effect on the percentage of double positive thymocytes (Fig. 23). The percentage of CD4 single positive population ($CD4^+CD8^-$) in TOC after 4 days, however, was greater than the percentage of those in a fresh neonatal thymus (Fig. 24). The percentage of $CD4^+$ thymocytes in TOC that received conditioned media from stimulated pDC was significantly increased compared with TOC that received conditioned media from unstimulated pDC (Fig. 25). Percentages of $CD4^+$ thymocytes in TOC that received conditioned media from unstimulated pDC were significantly decreased compared with TOC control (Fig. 25). When the percentage of CD8 single positive ($CD4^-CD8^+$) and double negative ($CD4^-CD8^-$) was examined, no significant different was found compared to these thymocyte populations in a fresh thymocytes (Fig. 26, 28 respectively). Treatment groups had no effect on the percentage of CD8 single positive ($CD4^-CD8^+$) and double negative ($CD4^-CD8^-$) (Fig. 27, 29 respectively).

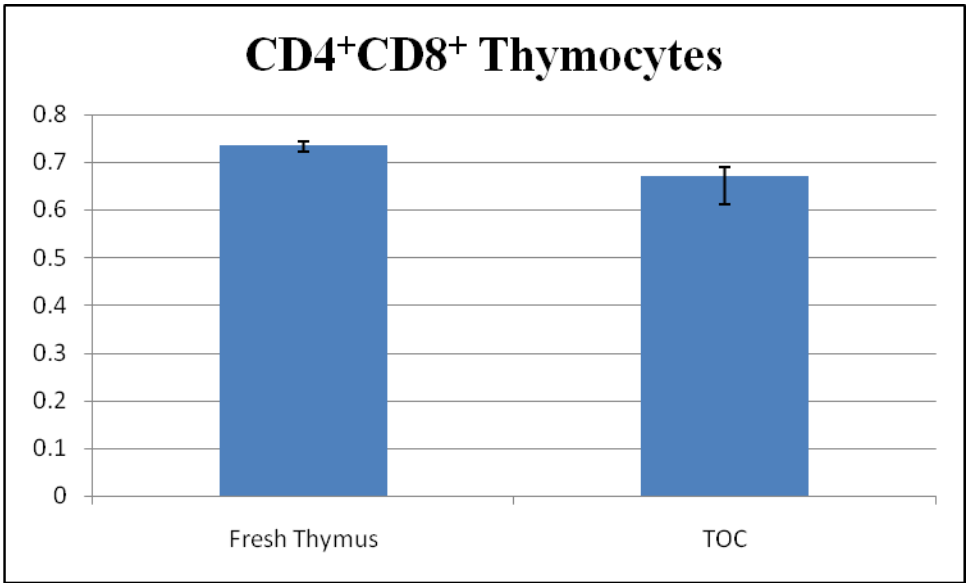

Figure 22. Percentage of double positive ($CD4^+CD8^+$) thymocytes in thymus organ culture compared with fresh thymus. The percentage of double positive ($CD4^+CD8^+$) thymocytes in 4 days of thymus organ culture was not significantly different from the percentage of these cells in fresh thymus. Bars represent the medians of 4 replicates. Antennae represent the interquartile range. Medians were compared using the Mann-Whitney U test, with $P<0.05$ considered significant.

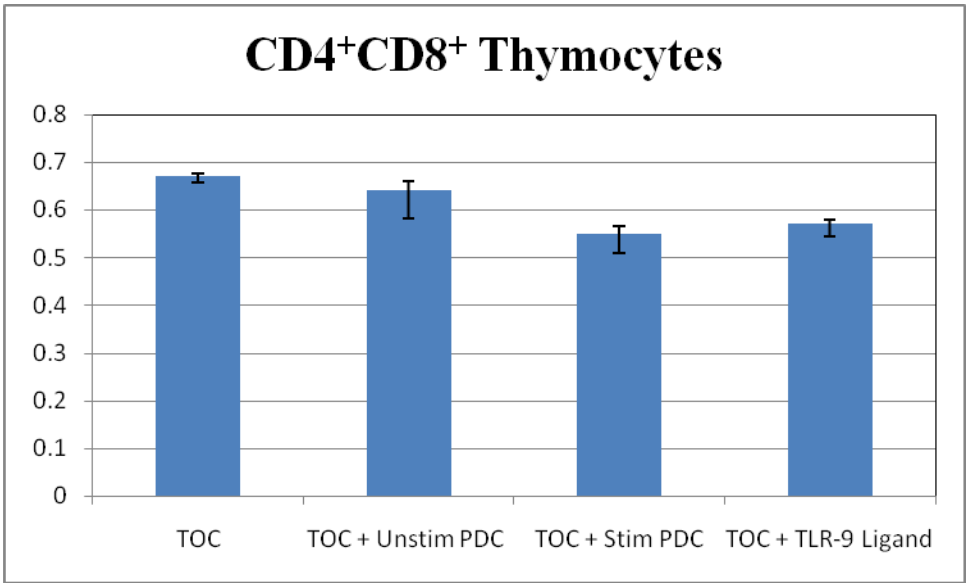

Figure 23. Treatment of TOC with supernatants from stimulated pDC, unstimulated pDC, or TLR9 ligand had no effect on the percentage of $CD4^{+}CD8^{+}$ thymocytes after 4 days in TOC. Bars represent the medians of 4 replicates. Antennae represent the interquartile range. Medians were compared using the Mann-Whitney U test, with $P<0.05$ considered significant.

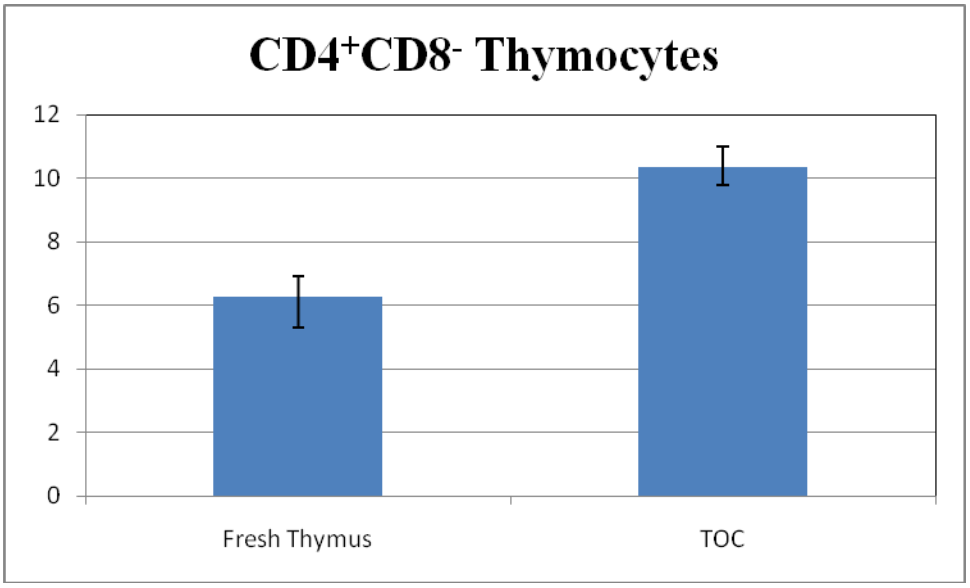

Figure 24. The percentage of single positive CD4 thymocytes ($CD4^+CD8^-$) after 4 days in thymus organ culture was significantly greater than the percentage of these cells in fresh thymus. Bars represent the medians of 4 replicates. Antennae represent the interquartile range. Medians were compared using the Mann-Whitney U test, with $P<0.05$ considered significant.

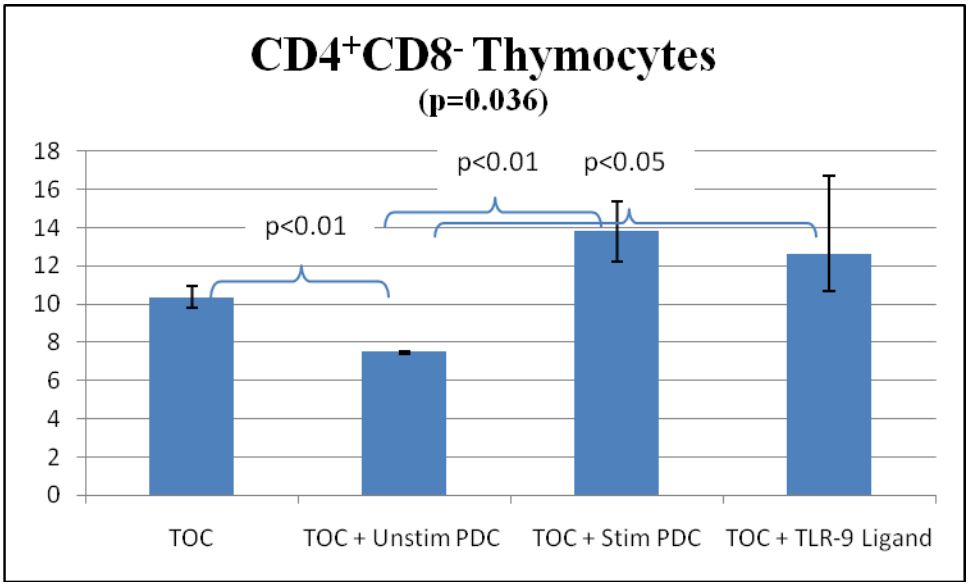

Figure 25. Treatment of TOC with supernatants from stimulated pDC, unstimulated pDC, or TLR9 ligand showed a significant reduction in CD4+CD8- cells in TOC treated with unstimulated pDC supernatant when compared with untreated TOC. In addition, $CD4^{+}CD8^{-}$ thymocyte percentages were significantly higher in TOC receiving stimulated pDC and TOC stimulated directly with TLR ligand when compared with TOC receiving unstimulated pDC supernatants. Bars represent the medians of 4 replicates. Antennae represent the interquartile range. Medians were compared using the Mann-Whitney U test, with $P<0.05$ considered significant.

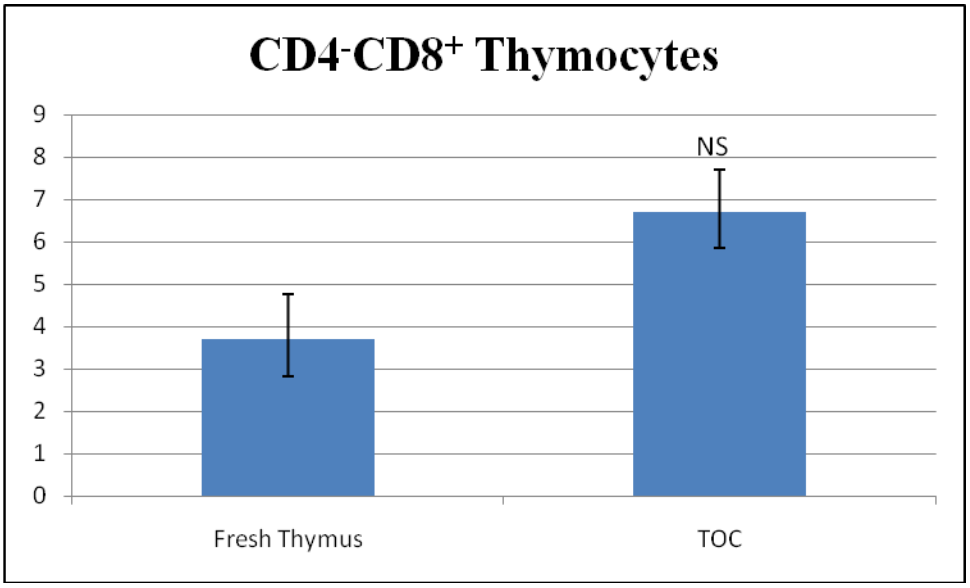

Figure 26. The percentage of single positive CD8 thymocytes ($CD4^{-}CD8^{+}$) after 4 days in thymus organ culture was not significantly different from the percentage of these cells in fresh thymus. Bars represent the medians of 4 replicates. Antennae represent the interquartile range. Medians were compared using the Mann-Whitney U test, with $P<0.05$ considered significant.

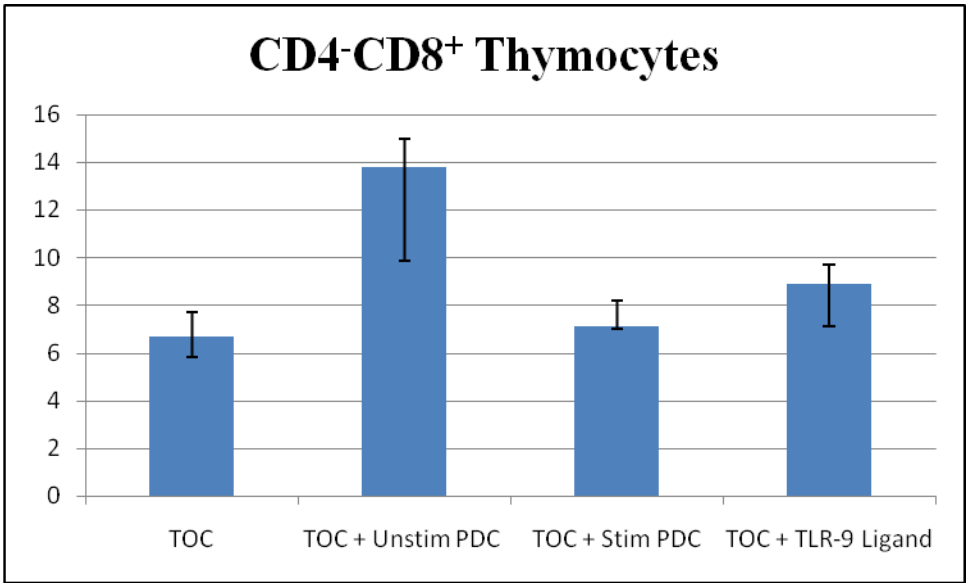

Figure 27. Treatment of TOC with supernatants from stimulated pDC, unstimulated pDC, or TLR9 ligand had no effect on the percentage of $CD4^{-}CD8^{+}$ thymocytes after 4 days in TOC. Bars represent the medians of 4 replicates. Antennae represent the interquartile range. Medians were compared using the Mann-Whitney U test, with $P<0.05$ considered significant.

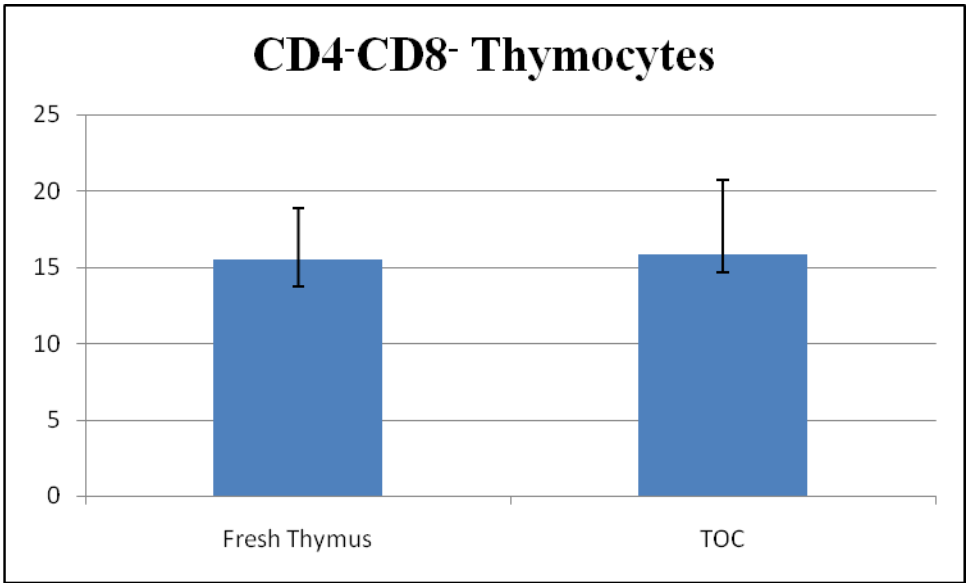

Figure 28. The percentage of double negative thymocytes (CD4-CD8-) after 4 days in thymus organ culture was not significantly different from the percentage of these cells in fresh thymus. Bars represent the medians of 4 replicates. Antennae represent the interquartile range. Medians were compared using the Mann-Whitney U test, with $P<0.05$ considered significant.

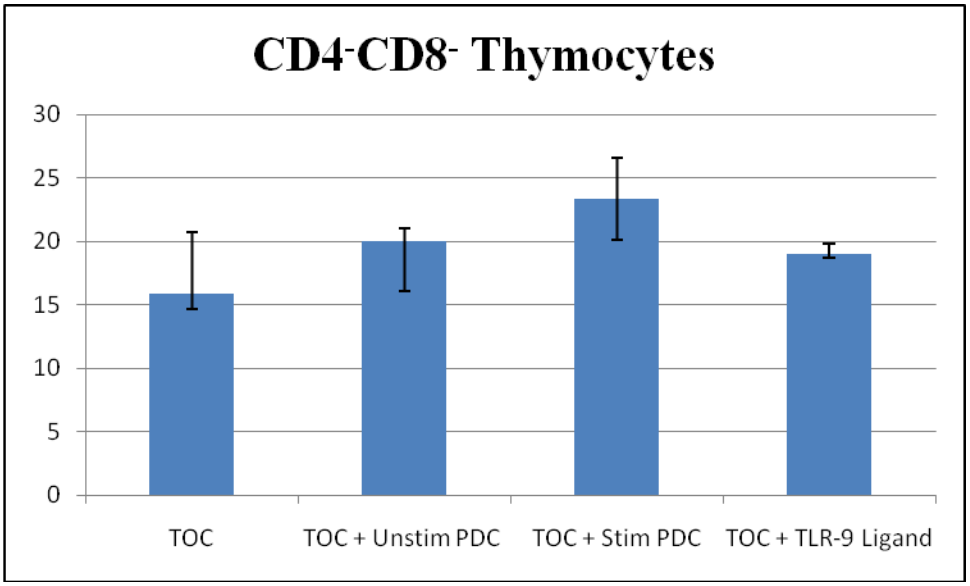

Figure 29. Treatment of TOC with supernatants from stimulated pDC, unstimulated pDC, or TLR9 ligand had no effect on the percentage of $CD4^{-}CD8^{-}$ thymocytes after 4 days in TOC. Bars represent the medians of 4 replicates. Antennae represent the interquartile range. Medians were compared using the Mann-Whitney U test, with $P<0.05$ considered significant.

We had earlier quantified cytokines TNF-α, IL-6, and IFN-α in the supernatants of media of stimulated pDC. To test our hypothesis that these cytokines in the supernatant of conditioned media altered thymopoiesis, we employed blocking antibodies to TNF-α, IL-6, and IFN-α. Anti-murine TNF-α, IL-6, and IFN-α were added to the supernatant of activated pDC and incubated prior to addition to TOC. The phenotype of fresh thymocytes and control TOC thymocytes was primarily double positive

(CD4+CD8+) at 75% and 68.5% respectively, as described previously. The treatment group with the lowest percentage of double positive (59%) was the TOC that received 70% conditioned media from stimulated pDC (Table 3) (Fig. 30). This same group also had the highest percentage of CD4 single positive thymocytes (15.6%) (Table 3) (Fig. 30). Treatment groups that received supernatant neutralized with blocking antibodies had higher percentages of double positive thymocytes than the group that received 70% conditioned media from stimulated pDC without blocking antibodies. The group that received anti-IFN-α, and the group that received all three antibodies had percentages of double positive thymocytes comparable to the control TOC group (Table 3) (Fig.30).

	DP ($CD4^+CD8^+$)	SP ($CD4^+CD8^-$)	SP ($CD4^-CD8^+$)	DN ($CD4^-CD8^-$)
Control fresh thymocytes	75%	6.1%	2.9%	17.1%
Control thymocytes 4 days	68.5%	11.8%	6.1%	13.6%
70% Cond Media Stim pDC	59%	15.6%	6.8%	18.5%
Block TNF-α	64.9%	10.5%	10.1%	14.6%
Block IL-6	65.2%	10.4%	7.7%	16.7%
Block IFN-α	69.99%	5.1%	12.5%	12.4%
Block TNF-α, IL-6, IFN-a	69.3%	8.6%	8.4%	13.7%

Table 3. Frequency of double positive, single positive, and double negative thymocytes in TOC, following neutralization of conditioned media with blocking antibodies against

TNF-α, IL-6, and IFN-α. A single blocking experiment was conducted; therefore, no statistical analysis was performed. However, there is a clear trend to indicate that blockade of IL-6, TNF-α, or IFN-α, or the simultaneous blockade of all three, to abrogate the effect of stimulated pDC on thymopoiesis.

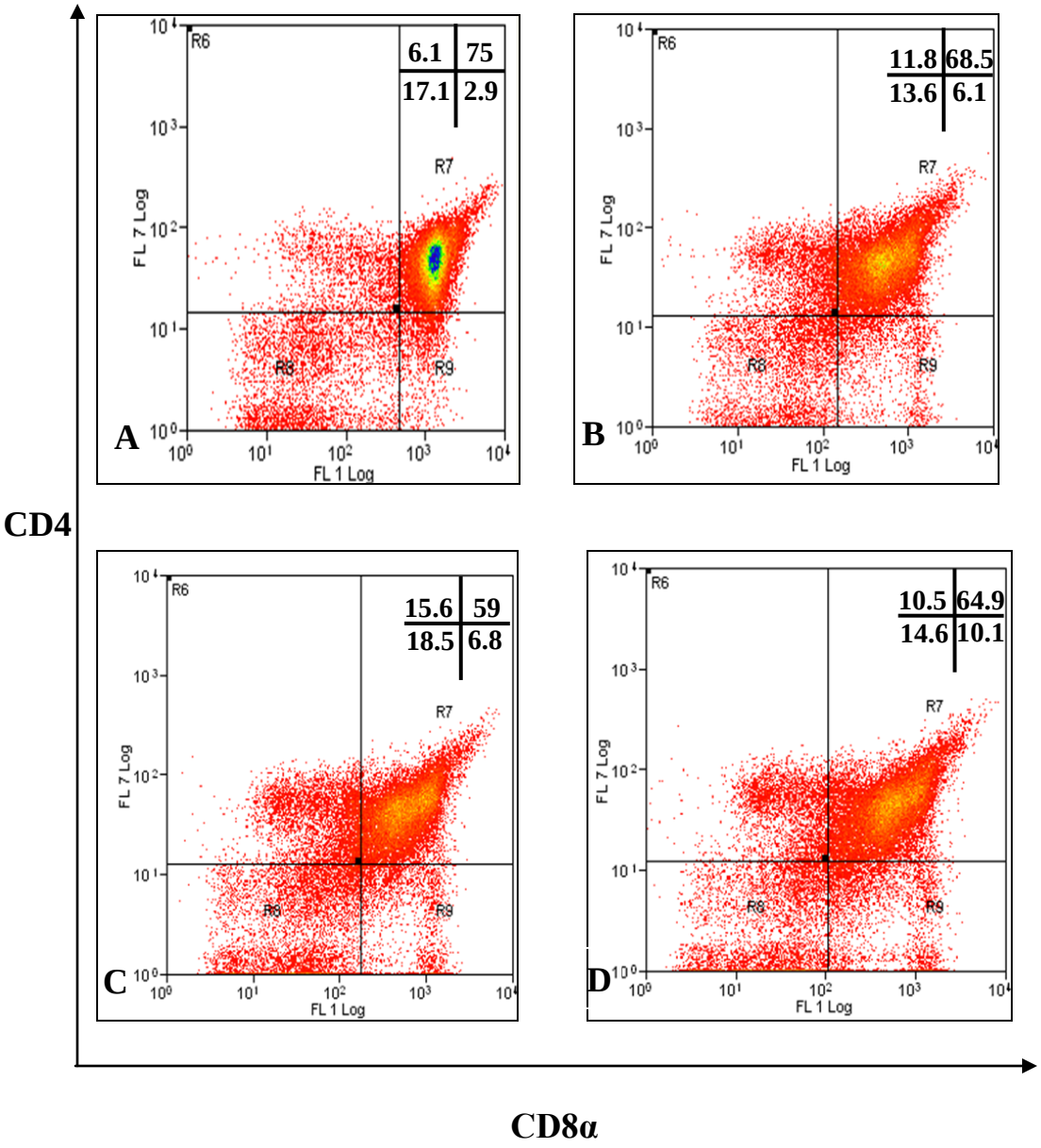

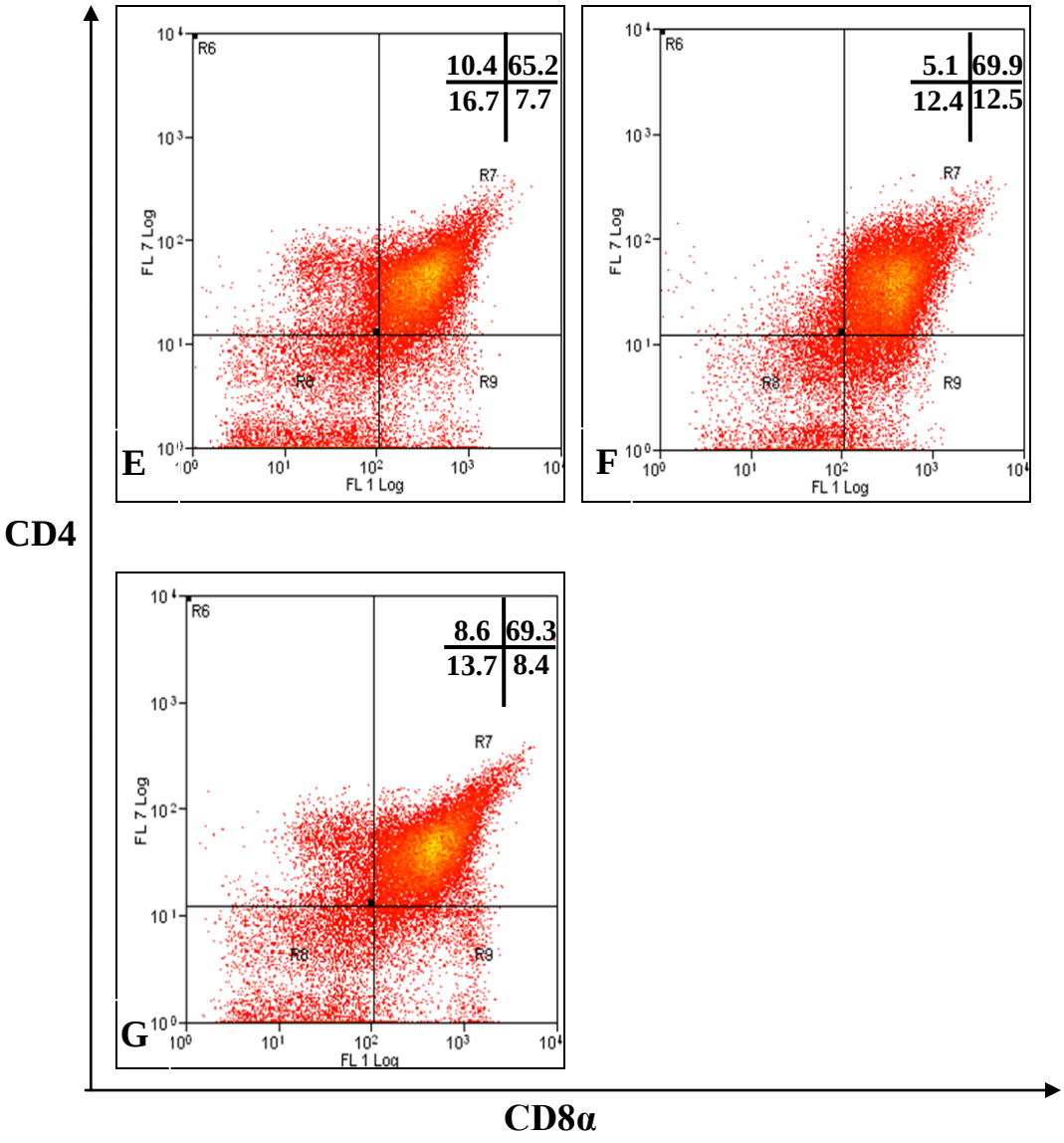

Figure 30. Addition of blocking antibodies TNF-α, IL-6, and IFN-α to TOC. **A.** fresh thymocytes, **B**. control thymocytes 4 days, **C**. TOC received 70% conditioned media from stimulated pDC, **D**. TOC received supernatant incubated with blocking antibody TNF-α, **E**. TOC received supernatant incubated with blocking antibody IL-6, **F**. TOC received supernatant incubated with blocking antibody IFN-α, **G**. TOC received supernatant incubated with blocking antibodies TNF-α, IL-6, and IFN-α.

Discussion

Plasmacytoid dendritic cells are the major producers of type I interferons and pro-inflammatory cytokines, and thereby regulate and activate numerous other cell types in the immune system. Their role in the thymus and effect on thymocytes is a subject continuing to be examined and not clearly defined. Type I interferons have been reported to inhibit early T cell development, exerting an effect on immature $CD4^{-}CD8^{-}$ $CD44^{+}CD25^{+}$ thymocytes (Lin *et al*., 1998). In the present study, we examined whether the products of stimulated pDC, type I interferon and pro-inflammatory cytokines, would inhibit thymopoiesis in thymus organ culture. Results of this study suggest that the secreted products in the supernatant of stimulated pDC have an effect on developing thymocytes. Our neutralization assay with blocking antibodies provided preliminary evidence to suggest that each of the evaluated cytokines had deleterious effects on thymopoiesis. Repeat experiments are needed to confirm that the trend is significant.

TOC treatment groups that received supernatant from stimulated pDC and those that received TLR9 ligand had significantly higher percentages of CD4 single positive ($CD4^{+}CD8^{-}$) thymocytes compared with TOC treatment groups that received supernatant from unstimulated pDC. No significant differences were observed between these same groups between percentages of double positive, CD8 single positive, and double negative thymocytes. These results suggest the accumulation of $CD4^{+}$ thymocytes may be due to an accelerated process of thymopoiesis or a disproportionate production of $CD4^{+}$ cells. However, it is also possible that the proportionate increase in single positive CD4 cells was the net effect of a global reduction in other thymocyte phenotypes, which were not

statistically significant when analyzed individually. The increase in double negative thymocytes in the TOC treatment groups that received conditioned supernatant from stimulated pDC and TLR9 ligand may indicate a perturbation in thymopoiesis, possibly a blockade from the double negative stage to the double positive stage. This interpretation would be consistent with the reported arrest of thymopoiesis at the DN phenotype induced by IFN-α (Lin *et al*., 1998).

A previous study found that pDC, activated by CpG or HIV-1, affected the development of $CD34^{+}CD1a^{-}$ thymic progenitor cells into T cells (Schmidlin *et al*., 2006). Additionally, the same study showed the addition of exogenous IFN-α blocked upregulation of cell surface markers associated with T cell development. The pDC stimulated in that study were generated in vitro by culturing $CD34^{+}CD1a^{-}$ thymic progenitor cells with the OP9 bone marrow stromal cell line (Schmidlin *et al*., 2006). In contrast, our study used native thymic pDC isolated from thymus tissue, which would be expected to provide a more realistic assessment of thymic pDC function.

CHAPTER 5

CONCLUSIONS

Dendritic cell biology has grown tremendously since the discovery and naming of these cells by Steinman and Cohn in 1973 (Steinman and Cohn, 1973). After more than three decades, dendritic cells have emerged as a key cell type in both innate and adaptive immunity, playing central roles in initiating antigen-specific T cell responses, induction of tolerance, and stimulation of other innate immune cells. Subsets of dendritic cells have been elucidated and localize in peripheral tissues, primary and secondary lymphoid tissues and blood. In the last ten years, one of the most unique lineages of dendritic cells, plasmacytoid dendritic cells, has gained increased interest for their large secretion of cytokines and ability to activate and promote other cell types. Plasmacytoid dendritic cells have emerged as key immune cells linking innate and adaptive immunity. There are numerous studies characterizing blood pDC, and pDC found in peripheral tissues in the human and the mouse. In the present study, we examined whether murine pDC isolated from the thymus modified thymopoiesis through their production of pro-inflammatory cytokines and type I interferons. Several experiments were employed to test this hypothesis: 1. Isolation of pDC from the murine thymus and determine the phenotype of these cells using specific dendritic cell markers; 2. Stimulation of thymic pDC and non-pDC cells and measurement of cytokine mRNA transcription and protein secretion; 3.

Measurement of phenotypic changes in developing thymocytes in culture with conditioned media from stimulated thymic pDC. Murine pDC were enriched from the thymuses of ICR mice through a novel serial process of mechanical disruption, enzymatic digestion, density gradient centrifugation and positive selection using mPDCA-1 mAb coated magnetic beads. Thymic pDC were stained with monoclonal antibodies specific to myeloid and plasmacytoid dendritic cells and analyzed by flow cytometry. We confirmed the phenotype of murine thymic pDC ($CD4^+CD11c^+CD123^+$m-$PDCA\text{-}1^+$) to be consistent with published reports of blood and peripheral pDC in the mouse (Bjorck, 2001; Schmitt *et al*., 2007). Two subsets of murine dendritic cells were identified in the low density cell fraction using cell surface markers CD11c and m-PDCA-1. Myeloid or conventional dendritic cells comprised approximately 4% of low density cells, and plasmacytoid dendritic cells made up almost 2% of low density cells. Our determination of the frequency of pDC in total thymocytes is consistent with published findings (Asselin-Paturel *et al*., 2003). We were able to use negative selection through FACS to enrich pDC, although this process provided a lesser yield of pDC and was lengthy and costly. However, despite the lower yield, a negative selection approach may reduce the likelihood of inadvertent activation of pDC during the enrichment process. Using the murine-specific pDC marker m-PDCA-1, we used positive selection using MACS, which gave us a greater yield of pDC per experiment compared to the yield of pDC using FACS, albeit at a moderately activated state based on basal levels of cytokine secretion.

In order to test our hypothesis that products of virus-activated pDC would inhibit or alter thymopoiesis, we first undertook several experiments to stimulate thymic pDC with TLR ligands. The results of our stimulation experiments revealed a pattern where

TNF-α and IL-6 transcripts peaked at 6 hours post stimulation, and protein levels of TNF-α, IL-6 and IFN-α were highest 24 hours post stimulation with TLR9 ligand. Amplification of the murine IFN-α mRNA target proved difficult due to the fact that the murine IFN-α gene has one exon. pDC were successfully stimulated, however, as they produced large quantities of TNF-α and IL-6 protein compared to non-pDC cells. Levels of cytokines produced by thymic pDC were found to be similar to published reports of stimulated pDC (Veckman and Julkunen, 2008). To test our overall hypothesis that virus-activated pDC interfere with thymopoiesis through their production of cytokines, we introduced the supernatant from stimulated and unstimulated pDC into a thymus organ culture system. The thymus organ cultures that received conditioned supernatant from stimulated pDC had a significant increase in percentage of $CD4^+CD8^-$ thymocytes and had lower numbers of $CD4^+CD8^+$ thymocytes when compared to thymus organ cultures that received supernatant from unstimulated pDC or TLR9 ligand alone. While the changes in other thymocyte populations were not statistically significant in the thymus organ cultures that received conditioned media from stimulated pDC, there was a trend of reduction in overall percentages of thymocytes, particularly the double positive phenotype, when compared with TOC that received conditioned media from unstimulated pDC or control groups. These results indicate that the secreted products of stimulated pDC alter thymopoiesis in this ex vivo model system. Further experiments are necessary to elucidate which cytokine or combination of cytokines exerts this effect on the events of normal thymocyte development. These data could help in the overall understanding of thymus dysfunction in the context of lentivirus infection, and lead to possible therapeutic options in the future.

While it is established that type I interferons comprise numerous roles in the overall immune response, their exact role in the thymus and effect on thymopoiesis is unclear. It has been reported that IFN-α has a detrimental effect on developing thymocytes. Lin *et al*. (1998) found IFN-α exerted toxic effects on the early stages of both B and T cell development and the overall cellularity of the thymus. Exogenously added IFN-α inhibited the IL-7-induced proliferation of triple negative (TN) thymocytes (Su *et al*., 1997), and impaired the upregulation of T-cell development cell surface markers on CD34+CD1a- thymic precursors (Schmidlin *et al*., 2006). The latter report made use of a coculture system of thymic progenitor cells and bone marrow stromal cell line to culture pDC and stimulate them with CpG or HIV-1 virus.

Large quantities of TNF-α and IL-6 produced by our stimulated pDC may also impair thymopoiesis as seen in our thymus organ culture studies. While both of these cytokines have a role in the growth of thymocytes (Ranges *et al*., 1988, Suda *et al*. 1990), IL-6 has also been reported to induce thymic atrophy and decrease thymic sjTRECs (Gruver and Sempowski, 2008; Sempowski *et al*., 2000). Thus, multiple products of activated pDC may contribute to the pathogenesis of thymus dysfunction in the murine TOC system.

While it is established that human pDC produce copious amounts of type I interferons, we surprisingly found that murine thymic pDC produced greater quantities of TNF-α and IL-6 protein compared with IFN-α protein. Thymic pDC may represent a unique lineage of pDC with a distinct role in the thymus through their production of TNF-α and IL-6. These two cytokines may indeed have a functional role in thymopoiesis but in large quantities prove toxic to the growth of developing thymocytes. Repeated

experiments are needed in additional strains of mice to determine if our findings were strain-specific. Asselin-Paturel *et al*. (2003) found 129Sv mice had higher frequencies of pDC in blood and spleen, when compared to C57BL/6 mice.

Overall, the preceding research shows that the secreted products of stimulated thymic pDC have a negative effect on the events of thymopoiesis. Lower percentages of double positive thymocytes were observed in TOC that received conditioned media from stimulated pDC, while these same TOC had significantly higher percentages of CD4 single positive thymocytes compared to other TOC treatment groups. The preliminary results of the neutralization assay with blocking antibodies to TNF-α, IL-6 and IFN-α lend support to the idea that the protective cytokines produced by pDC can also be harmful to natural physiological processes in large quantities or during a state of chronic activation. Further studies are necessary to confirm these findings and elucidate the specific product or combination of products secreted by thymic pDC that alter thymopoiesis. This basic mechanism could then be targeted therapeutically in conjunction with antiviral therapy to diminish overall thymus dysfunction.

BIBLIOGRAPHY

Akira, S., and Takeda, K. 2004. Toll-like receptor signaling. Nature Reviews Immunology 4:499-511.

Argyris, E.G., Pomerantz, R.J. 2004. HIV-1 Vif versus APOBEC3G: newly appreciated warriors in the ancient battle between virus and host. Trends in Microbiology 12(4):145-148.

Ashton-Rickardt, P.G. 2007. Studying T-cell repertoire selection using fetal thymus organ culture. Methods in Molecular Biology: Immunological Tolerance Methods and Protocols 380:171-184.

Asselin-Paturel, C., Boonstra, A., Dalod, M., Durand, I., Yessaad, N., Dezutter-Dambuyant, C., Vicari, A., O'Garra, A., Biron, C., Briere, F., Trinchieri, G. 2001. Mouse type I IFN-producing cells are immature APCs with plasmacytoid morphology. Nature Immunology 2(12):1144-1150.

Asselin-Paturel, C., Brizard, G., Pin, J.J., Briere, F., Trinchieri, G. 2003. Mouse strain differences in plasmacytoid dendritic cell frequency and function revealed by a novel monoclonal antibody. Journal of Immunology 171:6466-6477.

Baron, M.L., Gauchat, D., La Motte-Mohs, R., Kettaf, N., Abdallah, A., Michiels, T., Zuniga-Pflucker, J.C., Sekaly, R.P. 2008. TLR ligand-induced type I IFNs affect thymopoiesis. Journal of Immunology 180:7134-7146.

Barton, G.M., Kagan, J.C. 2009. A cell biological view of Toll-like receptor function: regulation through compartmentalization. Nature Reviews Immunology 9:535-542.

Barton, G.M. 2008. A calculated response: control of inflammation by the innate immune system. The Journal of Clinical Investigation 118(2):413-420.

Beaumont, C., Porcher, C., Picat, C., Nordmann, Y., Grandchamp, B. 1989. The mouse porphobilinogen deaminase gene. Structural organization, sequence, and transcriptional analysis. Journal of Biological Chemistry 264:14829-34.

Bendriss-Vermare, N., Barthelemy, C., Durand, I., Bruand, C., Dezutter-Dambuyant, C., Moulian, N., Berrih-Aknin, S., Caux, C., Trinchieri, G., Briere, F. 2001. Human thymus contains IFN-α-producing $CD11c^-$, myeloid $CD11c^+$, and mature interdigitating dendritic cells. Journal of Clinical Investigation 107(7):835-844.

Biron, C.A. 2001. Interferons α and β as immune regulators - a new look. Immunity 14:661-664.

Bjorck, P. 2001. Isolation and characterization of plasmacytoid dendritic cells from Flt3 ligand and granulocyte-macrophage colony-stimulating factor-treated mice. Blood 98(13):3520-3526.

Blasius, A.L., Giurisato, E., Cella, M., Schreiber, R.D., Shaw, A.S., Colonna, M. 2006. Bone marrow stromal cell antigen 2 is specific marker of type I IFN-producing cells in the naïve mouse, but a promiscuous cell surface antigen following IFN stimulation. Journal of Immunology 177:3260-3265.

Bowie, A.G., and Haga, I.R. 2005. The role of Toll-like receptors in the host response to viruses. Molecular Immunology 42:859-867.

Brinkmann, M.M., Spooner, E., Hoebe, K., Beutler, B., Ploegh, H.L., Kim, Y.M. 2007. The interaction between the ER membrane protein UNC93B and TLR3, 7, and 9 is crucial for TLR signaling. The Journal of Cell Biology 177(2):265-275.

Chehimi, J., Campbell, D.E., Azzoni, L., Bacheller, D., Papasavvas, E., Jerandi, K., Kostman, J., Trinchieri, G., Montaner, L.J. 2002. Persistent decreases in blood plasmacytoid dendritic cell number and function despite effective highly active antiretroviral therapy and increased blood myeloid dendritic cells in HIV-infected individuals. Journal of Immunology 168: 4796-4801.

Colonna, M., Trinchieri, G., Liu, Y.J. 2004. Plasmacytoid dendritic cells in immunity. Nature Immunology 5(12):1219-1226.

Conrad, C., Meller, S., Gilliet, M. 2009. Plasmacytoid dendritic cells in the skin: To sense or not to sense nucleic acids. Seminars in Immunology 21:101-109.

Cook, D.N., Pisetsky, D.S., Schwartz, D.A. 2004. Toll-like receptors in the pathogenesis of human disease. Nature Immunology 5(10):975-979.

Corcoran, L., Ferrero, I., Vremec, D., Lucas, K., Waithman, J., O'Keeffe, M., Wu, L., Wilson, A., Shortman, K. 2003. The lymphoid past of mouse plasmacytoid cells and thymic dendritic cells. Journal of Immunology 170:4926-4932.

Donaghy, H., Pozniak, A., Gazzard, B., Qazi, N., Gilmour, J., Gotch, F., Patterson, S. 2001. Loss of blood CD11c+ myeloid and CD11c- plasmacytoid dendritic cells in patients with HIV-1 infection correlates with HIV-1 RNA virus load. Blood 98(8): 2574-2576.

Dzionek, A., Sohma, Y., Nagafune,J., Cella, M., Colonna, M., Facchetti, F., Gunther,G., Johnston,I., Lanzavecchia,A., Nagasaka,T., Okada,T., Vermi,W., Winkels,G., Yamamoto,T., Zysk,M., Yamaguchi,Y., Schmitz,J. 2001. BDCA-2, a novel plasmacytoid dendritic cell-specific Type II C-type lectin, mediates antigen capture and is a potent inhibitor of Interferon α/β induction. Journal of Experimental Medicine 194(12):1823-1834.

Feldman, S., Stein, D., Amrute, S., Denny, T., Garcia, Z., Kloser, P., Sun, Y., Megjugorac, N., Fitzgerald-Bocarsly, P. 2001. Decreased interferon-α production in HIV-infected patients correlates with numerical and functional deficiencies in circulating type 2 dendritic cell precursors. Clinical Immunology 101(2):201-210.

Fitzgerald-Bocarsly, P. 2002. Natural interferon-α producing cells: The plasmacytoid dendritic cells. Biotechniques 33:S16-S29.

Fitzgerald-Bocarsly, P. Feng, D. 2007. The role of type I interferon production by dendritic cells in host defense. Biochimie 89:843-855.

Fonteneau, J.F., Larsson, M., Beignon, A.S., McKenna, K., Dasilva, I., Amara, A., Liu, Y.J., Lifson, J.D., Littman, D.R., Bhardwaj, N. 2004. Human immunodeficiency virus type 1 activates plasmacytoid dendritic cells and concomitantly induces the bystander maturation of myeloid dendritic cells. Journal of Virology 78(10):5223-5232.

Fuchsberger, M., Hochrein, H., O'Keeffe, M. 2005. Activation of plasmacytoid dendritic cells. Immunology and Cell Biology 83:571-577.

Gaulton, G.N., Scobie, J.V., Rosenzweig, M. 1997. HIV-1 and the thymus. AIDS 11(4):403-414.

Gilliet, M, Cao, W., Liu, Y.J. 2008. Plasmacytoid dendritic cells: sensing nucleic acids in viral infection and autoimmune diseases. Nature Reviews Immunology 8:594-606.

Grouard, G., Rissoan, M.C., Filgueira, L., Durand, I., Banchereau, J., Liu, Y.J. 1997. The enigmatic plasmacytoid T cells develop into dendritic cells with interleukin(IL)-3 and CD40-Ligand. Journal of Experimental Medicine 185(6):1101-1111.

Gruver, A.L., Sempowski, G.D. 2008. Cytokines, leptin, and stress-induced thymic atrophy. Journal of Leukocyte Biology 84:1-9.

Gurney, K.B., Colantonio, A.D., Blom, B., Spits, H., Uittenbogaart, C.H. 2004. Endogenous IFN-α production by plasmacytoid dendritic cells exerts an antiviral effect on thymic HIV-1 infection. Journal of Immunology 173:7269-7276.

Haller, O., Kochs, G., Weber, F. 2007. Interferon, Mx, and viral countermeasures. Cytokine & Growth Factor Reviews 18:425-433.

Harrt Meyers, J., Justement, S., Hallahan, C.W., Blair, E.T., Sun, Y.A., O'Shea, M.A., Roby, G., Kottilil, S., Moir, S., Kovacs, C.M., Chun, T.W., Fauci, A.S. 2007. Impact of HIV on cell survival and antiviral activity of plasmacytoid dendritic cells. PLoS ONE 2(5):e458.

Haynes, B.F., Market, M.L., Sempowski, G.D., Patel, D.D., Hale, L.P. 2000. The role of the thymus in immune reconstitution in aging, bone marrow transplantation, and HIV-1 infection. Annual Review of Immunology 18:529-560.

Hochrein, H., Schlatter, B., O'Keefe, M., Wagner, C., Schmitz, F., Schiemann, M., Bauer, S., Suter, M., Wagner, H. 2004. Herpes simplex virus type-1 induces IFN-α production via Toll-like receptor 9-dependent and –independent pathways. Proc. Natl. Acad. Sci. USA 101:11416-11421.

Hogquist, K.A. 2001. Assays of thymic selection. Methods in Molecular Biology 156:219 -232.

Ito, T., Kanzier, H., Duramad, O., Cao, W., Liu, Y.J. 2006. Specialization, kinetics, and repertoire of type I interferon responses by human plasmacytoid predendritic cells. Blood 107:2423-2431.

Janeway, C.A., Travers, P.,Walport, M., Shlomchik, M.J. 2005. Immunobiology: the immune system in health and disease. 6th Ed. Garland Science Publishing.

Janeway, C.A., Medzhitov, R. 2002. Innate immune recognition. Annual Review of Immunology 20:197-216.

Kadowaki, N., Ho, S., Antonenko, S., de Waal Malefyt, R., Kastelein, R.A., Bazan, F., Liu, Y.J. 2001. Subsets of human dendritic cell precursors express different toll-like receptors and respond to different microbial antigens. Journal of Experimental Medicine 194(6):863-869.

Katze, M.G., He, Y., Gale, M. 2002. Viruses and interferon: a fight for supremacy. Nature Reviews Immunology 2:675-687.

Kim, Y.M., Brinkmann, M.M., Ploegh, H.L. 2007. TLRs bent into shape. Nature Immunology 8:675-677.

Kim, Y.M., Brinkmann, M.M., Paquet, M., Ploegh, H.L. 2008. UNC93B1 delivers nucleotide-sensing toll-like receptors to endolysosomes. Nature 452:234-239.

Kolenda-Roberts, H.M. 2006. Cytokine profiles and viral replication within the thymuses of neonatally feline immunodeficiency virus-infected cats. Dissertation; University of Florida.

Kolenda-Roberts, H.M., Kuhnt, L.A., Jennings, R.N., Mergia, A., Gengozian, N., Johnson, C.M. 2007. Immunopathogenesis of feline immunodeficiency virus infection in the fetal and neonatal cat. Frontiers in Bioscience 12:3668-3682.

Latz, E., Shoenemeyer, A., Visintin, A., Fitzgerald, K.A., Monks, B.G., Knetter, C.F., Lien, E., Nilsen, N.J., Espevik, T., Golenbock, D.T. 2004. TLR9 signals after translocating from the ER to CpG DNA in the lysosome. Nature Immunology 5(2):190-198.

Lennert, K., Remmele, W. 1958. Karyometric research on lymph node cells in man. I. Germinoblasts, lymphoblasts and lymphocytes. Acta Haematologica 19:99-113. (in German)

Lin, Q., Dong, C., Cooper, M.D. 1998. Impairment of T and B cell development by treatment with Type I Interferon. Journal of Experimental Medicine 187(1):79-87.

Liu, Y.J. 2005. IPC: Professional type 1 interferon-producing cells and plasmacytoid dendritic cell precursors. Annual Review of Immunology 23:275-306.

Lotz, M., Jirik, F., Kabouridis, P., Tsoukas, C., Hirano, T., Kishimoto, T., Carson, D.A. 1988. B cell stimulating factor 2/Interleukin 6 is a costimulant for human thymocytes and T lymphocytes. Journal of Experimental Medicine 167(3):1253-1258.

Luciano, L. 2002. Southern discomfort-coping with HIV/AIDS in the South poses challenges. Kaisernetwork. www.adph.org.

Marshak-Rothstein, A. 2006. Toll-like receptors in systemic autoimmune disease. Nature Reviews Immunology 6:823-835.

McCune, J.M. 1997. Thymic function in HIV-1 disease. Seminars in Immunology 9:397-404.

McKenna, K., Beignon, A.S., Bhardwaj, N. 2005. Plasmacytoid dendritic cells: linking innate and adaptive immunity. Journal of Virology 79(1):17-27.

Meissner, E.G., Duus, K.M., Loomis, R., D'Agostin, R., Su, L. 2003. HIV-1 replication and pathogenesis in the human thymus. Current HIV Research 1(3):275-285.

Moynagh, P.N. 2005. TLR signaling and activation of IRFs: revisiting old friends from the NF-κB pathway. Trends in Immunology 26(9):469-476.

Muller-Trutwin, M., and Hosmalin, A. 2005. Role of plasmacytoid dendritic cells in anti-HIV innate immunity. Immunology and Cell Biology 83(5):578-585.

Naik, S.H., Corcoran, L.M., Wu, L. 2005. Development of murine plasmacytoid dendritic cell subsets. Immunology and Cell Biology 83:563-570.

Nakano, H., Yanagita, M., Gunn, M.D. 2001. CD11c+B220+Gr-1+ cells in mouse lymph nodes and spleen display characteristics of plasmacytoid dendritic cells. Journal of Experimental Medicine 194(8):1171-1178.

Okada, T., Lian, Z.X., Naiki, M., Ansari, A.A., Ikehara, S., Gershwin, M.E. 2003. Murine thymic plasmacytoid dendritic cells. European Journal of Immunology 33:1012-1019.

Omatsu, Y., Iyoda, T., Kimura, Y., Maki, A., Ishimori, M., Toyama-Sorimachi, N., Inaba, K. 2005. Development of murine plasmacytoid dendritic cells defined by increased expression of an inhibitory NK receptor, Ly49Q. Journal of Immunology 174:6657-6662.

Orandle, M.S., Papadi, G.P., Bubenik, L.J., Dailey, C.I., Johnson, C.M. 1997. Selective thymocyte depletion and immunoglobulin coating in the thymus of cats infected with feline immunodeficiency virus. AIDS Research and Human Retroviruses 13(7):611-20.

Patterson, S., Rae, A., Hockey, N., Gilmour, J., Gotch, F. 2001. Plasmacytoid dendritic cells are highly susceptible to human immunodeficiency virus type 1 infection and release infectious virus. Journal of Virology 75(14):6710-6713.

Pitha, P.M., Kunzi, M.S. 2007. Type I Interferon: the ever unfolding story. Current topics in microbiology and immunology 316:41-70.

Ramsdell, F., Zuniga-Pflucker, J.C., Takahama, Y. 2006. In vitro systems for the study of T cell development: Fetal thymus organ culture and OP9-DL1 Cell Coculture. Current Protocols in Immunol*ogy* 3.18.1-3.18.18

Ranges, G. E., Zlotnik, A., Espevik, T., Dinarello, C.A., Cerami, A., Palladino, M.A. 1988. Tumor necrosis factor α/Cachectin is a growth factor for thymocytes. Journal of Experimental Medicine 167:1472-1478.

Res, P.C.M., Couwenberg, F., Vyth-Dreese, F.A., Spits, H. 1999. Expression of pTα mRNA in a committed dendritic cell precursor in the human thymus. Blood 94(8):2647-2657.

Rossi, M., Young, J.W. 2005. Human dendritic cells: Potent antigen-presenting cells at the crossroads of innate and adaptive immunity. Journal of Immunology 175:1373-1381.

Saitoh, S.I. and Miyake, K. 2009. Regulatory molecules required for nucleotide-sensing Toll-like receptors. Immunological Reviews 227:32-43.

Samuel, C.E. 2001. Antiviral actions of interferons. Clinical Microbiology Reviews 14(4):778-809.

Schiller, M., Metze, D., Luger, T.A., Grabbe, S., Gunzer, M. 2006. Immune response modifiers – mode of action. Experimental Dermatology 15:331-341.

Schmidlin, H., Dontje, W., Groot, F., Ligthart, S.J., Colantonio, A.D., Oud, M.E., Schilder-Tol, E.J., Spaargaren, M., Spits, H., Uittenbogarrt, C.H., Blom, B. 2006. Stimulated plasmacytoid dendritic cells impair human T-cell development. Blood 108(12):3792-3800.

Schmidt, B., Ashlock, B.M., Foster, H., Fujimura, S.H., Levy, J.A. 2005. HIV-infected cells are the major inducers of plasmacytoid dendritic cell interferon production, maturation, and migration. Virology 343:256-266.

Schmidt, B., Scott, I., Whitmore, R.G., Foster, H., Fujimura, S., Schmitz, J., Levy, J.A. 2004. Low-level HIV infection of plasmacytoid dendritic cells: onset of cytopathic effects and cell death after PDC maturation. Virology 329:280-288.

Schmitt,N., Cumont,M.C., Nugeyre,M.T., Hurtrel,B., Barre-Sinoussi,F. Scott-Algara,D., Israel,N. 2007. Ex vivo characterization of human thymic dendritic cell subsets. Immunobiology 212(3):167-177.

Sempowski, G.D., Hale, L.P., Sundy, J.S., Massey, J.M., Koup, R.A., Douek, D.C., Patel, D.D., Haynes, B.F. 2000. Leukemia inhibitory factor, Oncostatin M, IL-6, and Stem cell factor mRNA expression in human thymus increases with age and is associated with thymic atrophy. The Journal of Immunology 164:2180-2187.

Siegal, F.P., Fitzgerald-Bocarsly, P., Holland, B.K., Shodell, M. 2001. Interferon-α generation and immune reconstitution during antiretroviral therapy for human immunodeficiency virus infection. AIDS 15:1603-1612.

Silverman, R.H. 2007. A scientific journey through the 2-5A/RNase L system. Cytokine & Growth Factor Reviews 18:381-388.

Soumelis, V., Scott, I., Gheyas, F., Bouhur, D., Cozon, G., Cotte, L., Huang, L., Levy, J.A., Liu, Y.J. 2001. Depletion of circulating natural type 1 interferon-producing cells in HIV-infected AIDS patients. Blood 98(4):906-912.

Steinman, R.M., Cohn, Z.A. 1973. Identification of a novel cell type in peripheral lymphoid organs of mice.I. Morphology, quantitation, tissue distribution. Journal of Experimental Medicine 137:1142-1162.

Steinman, R.M., Hemmi, H. 2006. Dendritic cells: Translating innate to adaptive immunity. Current topics in Microbiology and Immunology 311:17-58.

Strausberg, R.L., Feingold, E.A., Grouse, L.H. 2002. Generation and initial analysis of more than 15,000 full-length human and mouse cDNA sequences. Proc. Natl. Acad. Sci. USA 99:16899-16903.

Su, D.-M., Wang, J., Lin, Q., Cooper, M.D., Watanabe, T. 1997. Interferons α/β inhibit IL-7-induced proliferation of $CD4^-CD8^-CD3^-CD44^+CD25^+$ thymocytes, but do not inhibit that of $CD4^-CD8^-CD3^-CD44^-CD25^-$ thymocytes. Immunology 90:543-549.

Suda, T., Murray, R., Guidos, C., Zlotnik, A. 1990. Growth-promoting activity of IL-1α, IL-6, and tumor necrosis factor-α in combination with IL-2, IL-4 or IL-7 on murine thymocytes. Journal of Immunology 144:3039-3045.

Taniguchi, T., Ogasawara, K., Takaoka, A., Tanaka, N. 2001. IRF family of transcription factors as regulators of host disease. Annual Review of Immunology 19:623-55.

Theofilopoulos, A.N., Baccala, R., Beutler, B., Kono, D.H. 2005. Type I Interferons (α/β) in immunity and autoimmunity. Annual Review of Immunology 23:307-36.

Veckman, V. Julkunen, I. 2008. Streptococcus pyogenes activates human plasmacytoid and myeloid dendritic cells. Journal of Leukocyte Biology 83:296-304.

Vidalain, P.O., Laine, D., Zaffran, Y., Azocar, O., Servet-Delprat, C., Wild, T.F., Rabourdin-Combe, C., Valentin, H. 2002. Interferons mediate terminal differentiation of human cortical thymic epithelial cells. Journal of Virology 76(13):6415-6424.

von Ashen, N., Oellerich, M., Schutz, E. 2000. A method for homogeneous color-compensated genotyping of factor V (G1691A) and methylenetetrahydrofolate reductase (C677T) mutations using real-time multiplex fluorescence PCR. *Clinical Biochemistry* 33:535-539.

Wang, C., Gao, D., Vaglenov, A., Kaltenboeck, B. 2004. One-step real-time duplex reverse transcription PCRs simultaneously quantify analyte and housekeeping gene mRNAs. Biotechniques 36(3):508-519.

Ware, C.F. 2003. The TNF Superfamily. Cytokine & Growth Factor Reviews 14:181-184.

Ware, C.F. 2008. The TNF Superfamily-2008. Cytokine & Growth Factor Reviews 19:183-186.

Ye, P., Kirschner, D.E., Kourtis, A.P. 2004. The thymus during HIV disease: Role in pathogenesis and in immune recovery. Current HIV Research 2(2):177-183.

Yonezawa, A., Morita, R., Takaori-Kondo, A., Kadowaki, N., Kitawaki, T., Hori, T., Uchiyama, T. 2003. Natural alpha interferon-producing cells respond to human immunodeficiency virus type 1 with alpha interferon production and maturation into dendritic cells. Journal of Virology 77(6):3777-3784.